

# The $\eta$ Chamaleontis Cluster: Origin in the Sco-Cen OB Association

Eric E. Mamajek<sup>1,2,3</sup>, Warrick A. Lawson<sup>1</sup> and Eric D. Feigelson<sup>4</sup>

## ABSTRACT

A young, nearby compact aggregate of X-ray emitting pre-main sequence stars was recently discovered in the vicinity of  $\eta$  Chamaleontis (Mamajek, Lawson & Feigelson 1999, ApJ, 516, L77). In this paper, we further investigate this cluster: its membership, its environs and origins. *ROSAT* High-Resolution Imager X-ray data for the cluster's T Tauri stars show high levels of magnetic activity and variability. The cluster has an anomalous X-ray luminosity function compared to other young clusters, deficient in stars with low, but detectable X-ray luminosities. This suggests that many low-mass members have escaped the surveyed core region. Photographic photometry from the USNO-A2.0 catalog indicates that additional, X-ray-quiet members exist in the cluster core region. The components of the eclipsing binary RS Cha, previously modeled in the literature as post-main sequence with discordant ages, are shown to be consistent with being coeval pre-MS stars.

We compute the Galactic motion of the cluster from *Hipparcos* data, and compare it to other young stars and associations in the fourth Galactic quadrant. The kinematic study shows that the  $\eta$  Cha cluster, as well as members of the TW Hya association and a new group near  $\epsilon$  Cha, probably originated near the giant molecular cloud complex that formed the two oldest subgroups of the Sco-Cen OB association roughly 10-15 Myr ago. Their dispersal is consistent with the velocity dispersions seen in giant molecular clouds. A large H I filament and dust lane located near  $\eta$  Cha has been identified as part of a superbubble formed by Sco-Cen OB winds and supernova remnants. The passage of the superbubble may have terminated star-formation in the  $\eta$  Cha cluster and dispersed its natal molecular gas.

*Subject headings:* Galaxy: open clusters and associations: individual ( $\eta$  Chamaleontis, Sco OB2, TW Hya,  $\epsilon$  Chamaleontis), stars: kinematics, stars: pre-main sequence, X-rays: stars

---

<sup>1</sup>School of Physics, University College, University of New South Wales, Australian Defence Force Academy, Canberra ACT 2600, Australia

<sup>2</sup>J. William Fulbright Fellow

<sup>3</sup>Current address: Steward Observatory, Department of Astronomy, University of Arizona, 933 N. Cherry Ave., Tucson AZ 85721, USA

<sup>4</sup>Department of Astronomy & Astrophysics, Pennsylvania State University, University Park, PA 16802, USA

## 1. Introduction

Intermediate-age pre-main sequence (pre-MS) stars (ages of  $\sim 5 - 30$  Myr) with established distances and ages are rare in the astronomical literature (Herbig 1978). Low-mass stars ( $0.1 - 3 M_{\odot}$ ) in this age range are predominantly past their active classical T Tauri phase, and are usually called weak-lined T Tauri stars (WTTs) or post-T Tauri stars (Martín 1997). Nearby stars ( $d < 150$  pc) in this age range are especially important for studies of stellar angular momentum evolution, stellar multiplicity, the evolution of young and luminous brown dwarfs and planets, and the evolution and longevity of circumstellar disks (e.g. Beckwith & Sargent 1996, Bouvier, Forestini & Allain 1997, Brandner & Koehler 1998, Low et al. 1999, Jayawardhana et al. 1999, Béjar et al. 1999). It is particularly valuable to studies of these issues to have samples of nearby, coeval, codistant stars in this age range.

Coronal X-ray emission (or more precisely, the ratio  $L_x/L_{bol}$ ) is elevated 1 – 3 orders of magnitude above main sequence levels in low-mass stars throughout the pre-MS phase (e.g., Briceño et al. 1997). Pointed X-ray observations of nearby active star-forming molecular clouds, where the bulk of the stars have modeled ages of  $< 2$  Myr, have identified many new weak-lined T Tauri stars missed by previous surveys (in Chamaeleon I (Feigelson et al. 1993), Taurus-Auriga (e.g. Strom & Strom 1994), and other active star-forming regions). Copious numbers of older pre-MS stars have been found in star clusters such as the 30 – 50 Myr-old clusters IC 2602 and IC 2391 (Randich et al. 1995, Stauffer et al. 1997), around the Orion molecular clouds ( $< 7$  Myr, Alcalá, Chavarría-K. & Terranegra 1998) and associated with Gould’s Belt ( $< 30$  Myr, Guillout et al. 1998). Hundreds of isolated pre-MS and ZAMS stars have been discovered with X-ray telescopes, particularly the *ROSAT* All-Sky Survey (RASS, see reviews by Neuhäuser 1999 and Feigelson & Montmerle 1999), and thus provides an excellent means for locating older WTT stars which may no longer be proximate to their parent molecular cloud. Two stellar associations with X-ray-selected samples of WTTs with ages around 5 – 20 Myr lie nearby: the Sco OB2 (Sco-Cen) association at  $d \simeq 110 - 150$  pc (e.g., de Zeeuw et al. 1999, Preibisch & Zinnecker 1999) and the TW Hya T Association at  $d \simeq 50$  pc (Webb et al. 1999).

Last year, a new, nearby stellar aggregate was added to the list: the  $\eta$  Chamaeleontis cluster (Ma-

majek et al. 1999, hereafter Paper I) with age  $t \approx 8$  Myr. The new cluster has  $d = 97$  pc, and contains 13 known members with masses  $0.1 - 3 M_{\odot}$  within a very small region (0.2 square degree) of sky. The cluster was discovered with a *ROSAT* High Resolution Imager (HRI) pointing of a tight group of 4 RASS X-ray sources previously established to be WTTs (Alcala et al. 1995, Covino et al. 1997). The low-mass X-ray-discovered stars have the lithium and  $H\alpha$  spectral signatures of WTT stars and are clustered around several intermediate-mass stars including the  $V = 5.5$  B8V star  $\eta$  Cha, and the  $V = 6$ , A8V+A8V double-lined, eclipsing binary RS Cha. Paper I announced the group as the fourth nearest open cluster to the Sun and the second nearest grouping of pre-MS stars after the TW Hya Association.

Since then, three additional candidate groups in the Sun’s neighborhood have been announced: the Carina-Vela group (a possible extension of Sco OB2; Makarov & Urban 2000) the “Tucanae Association” (Zuckerman & Webb 2000), a new association of  $\sim 30$ -Myr-old post-T Tauri stars in Horologium (Torres et al. 2000), and a small group of T Tauri stars associated with the isolated MBM 12 cloud (Hearty et al. 2000). As with the  $\eta$  Cha cluster, these new groups will require further study to piece together the recent star-formation history of the solar neighborhood, as well as investigate the dynamics of disintegrating star clusters..

The present paper discusses the properties and origins of the  $\eta$  Cha cluster in detail. The X-ray data for cluster members is presented in Section 2. Section 3 gives preliminary evidence for the existence of additional cluster members in the core region. Section 4 compares the  $\eta$  Cha cluster to other open clusters. In Section 5, we investigate the kinematics and origins of the  $\eta$  Cha cluster with respect to other young stars in the 4th Galactic quadrant. We argue that the  $\eta$  Cha cluster, the Sco-Cen OB association, the TW Hya Association, and a group of young stars near  $\epsilon$  Cha, likely formed in or near the same giant molecular cloud complex 5 – 15 Myr ago. Section 6 discusses the interstellar medium (ISM) in the direction of the  $\eta$  Cha cluster and strengthens the claim for a kinematic origin in Sco-Cen. Our findings are summarized in Section 7. Appendix A details the kinematics of the  $\eta$  Cha cluster, the TW Hya association, the  $\epsilon$  Cha group, and the Sco-Cen association. Appendix B presents notes on individual  $\eta$  Cha cluster members. Particular attention is paid to the eclipsing binary RS

Cha, which we find to be consistent with being two pre-MS A stars, but which has been modelled in previous literature as a non-coeval post-main sequence system.

## 2. X-ray Observations

### 2.1. Source Identifications

We observed the  $\eta$  Cha region with the HRI (Zombeck et al. 1995) on board the *ROSAT* satellite (Trümper 1983) for about 12 hours in 32 segments spread over several months in 1997. Exposures were obtained during 4 satellite orbits over April 26 – 29, 14 orbits distributed between September 11 and October 8, and during a more concentrated group of 17 orbits in October 26 – 29. These data were analyzed within the IRAF/PROS (version 2.5.1) software system (Smithsonian Astrophysical Observatory 1998). The image received from the *ROSAT* Standard Analysis Software System (SASS version 7) showed prominent sources, each showing identical structure distributed over  $15''$  due to incorrect satellite aspect solutions. To alleviate this problem, the images were divided into orbital intervals, centroids fitted to the brightest near-axis source, and the images aligned and merged (Harris et al. 1998). The reconstructed image, shown in Figure 1, is improved with residual distortions of a few arcseconds. About 1.5 hours of data were lost in this realignment process giving a net exposure of 41.7 ks.

Sources were located in the merged image with a cell detection algorithm within the IRAF/PROS software system, where square cells with sizes  $6'' \times 6''$  and  $24'' \times 24''$  are passed along the image to find peaks exceeding signal-to-noise ratio  $S/N = 3$ . This ratio is computed using Poisson statistics after subtraction of a local background level and was confirmed manually using a global background level. The centroid positions of each peak was located with a likelihood ratio statistic. Satellite boresight aspect errors frequently translate *ROSAT* images by several arcseconds. This was corrected by aligning eight strong X-ray source positions with their corresponding optical star positions, resulting in a good fit with boresight residuals in a range  $\pm 2''$ . With the exception of RECX 12 where the right ascension is unreliable due to off-axis telescope coma, the statistical X-ray positional uncertainties are  $1'' - 3''$  and the total uncertainties are about  $2'' - 4''$ .

The resulting 12 X-ray sources and their proper-

ties derived from the HRI data are listed in Table 1. Following Paper I, these sources are denoted by their *ROSAT*  $\eta$  Chamaeleon X-ray (RECX) number. In columns 2 and 3, counts in the time-integrated image are measured in circles ranging from  $20'' - 57''$  diameter, depending on the off-axis angle, after removal of a constant background value of 0.0638 counts per square arc second. Uncertainties are based only on counting statistics. The effective exposure time is the detector live time of 41.7 ks corrected for location-dependent detector quantum efficiency variations, telescope vignetting, and point spread function scattering following SASS procedures. This calculation is not optimized to achieve the high signal-to-noise ratio; e.g., the weakest source, RECX 9, shows  $S/N = 2$  in Table 1 but has  $S/N = 4$  when a smaller extraction circle is used.

In column 4, luminosities are estimated using a distance of 97 pc (Paper I) and the conversion  $1 \text{ count ks}^{-1} = 3 \times 10^{-14} \text{ erg s}^{-1} \text{ cm}^{-2}$  in the 0.1–2 keV band. Derived from a convolution of Raymond-Smith thermal plasma source spectra with the telescope and instrument response functions using the W3PIMMS software, this conversion is accurate to  $\pm 0.2$  in  $\log L_X$  for any combination of source temperatures  $kT > 0.2$  keV and column densities  $N_H < 1 \times 10^{20} \text{ cm}^{-2}$ . Note that this  $L_X$  applies only to the 0.1–2 keV band at the source, and not the luminosity emitted over all energies which can be substantially larger.

Stellar counterparts (column 5) were sought from the SIMBAD database, Hubble Space Telescope Guide Star Catalog (version 1.2), United States Naval Observatory PMM catalog (USNO-A2.0), and the Digitized Sky Survey (DSS). The offset between the X-ray source and stellar counterpart in column 6 is based on optical positions given in Paper I. The final columns summarizes X-ray variability characteristics of the sources (see below), and USNO  $B_J$  and  $F$  photometry (see §3.2 for discussion on USNO magnitudes)

In addition to these  $S/N > 3$  sources, potential weak sources with lower  $S/N$  or found only in a limited pulse height channel range (PHA = 3 – 8) where background rates are lower (David et al. 1997) were examined on both the HRI image and DSS. One additional source was found: a marginal X-ray source at the extreme northern edge of the image near the star GSC 9398\_0105 with  $B_J = 12.3$ ,  $F = 11.6$ . For its blue color, GSC 9398\_0105 is a few magnitudes too faint to be a member of the cluster, and we do not assign it an RECX number.

## 2.2. X-ray spectra and variability

The HRI has a limited spectral response capable of providing a single hardness ratio within the 0.1–2 keV band (Prestwich et al. 1998). Due to spatial variations in the detector response and changes in the detector high voltage level made between segments of our observation, we do not attempt a quantitative analysis. But qualitative examination of the pulse height data shows a distinct trend. The brightest source, RECX 1, is also the hardest. Sources with intermediate luminosities around  $\log L_X \simeq 30.0 \text{ erg s}^{-1}$ , have intermediate hardness ratios consistent with thermal emission in the range  $0.2 < kT < 1 \text{ keV}$ . The fainter sources with  $\log L_X \simeq 29.0 \text{ erg s}^{-1}$  have the softest spectra. This trend is seen in T Tauri and other young star samples, and can be explained by relatively simple models of plasma heated by magnetic reconnection in loops near the stellar surface (Preibisch 1997).

As the X-ray emission from young late-type stars is known to be highly variable due to flares and other manifestations of magnetic activity, the photon arrival times were examined. Column 7 of Table 1 summarises the presence and degree of variability. “Yes” indicates that the source is variable at a  $>99\%$  confidence level using nonparametric one-sample Kolmogorov-Smirnov and von Mises tests against the hypothesis of a constant source, “Possible” indicates 90%–99% probability from one or both tests, and “No” indicates consistency with a constant count rate. The approximate minimum and maximum levels in HRI counts  $\text{ks}^{-1}$  seen in the light curves appear in parentheses.

Figure 2 shows the more dramatic changes seen in the seven variable sources. Factors of 2–4 jumps of flux on timescales ranging from 0.5 to  $>2$  days are seen. Fluxes often exhibit a factor of 3–7 range over the entire observation with peak luminosities between  $10^{30.1-30.9} \text{ erg s}^{-1}$ . The light curves give the impression of individual powerful flares superposed on more moderately variable emission. The best-recorded event occurred in RECX 8 (= RS Cha) and shows a decay timescale of  $\sim 0.5$  days.

## 2.3. Anomalous X-ray luminosity function

While the X-ray properties of the  $\eta$  Cha stars are similar in most respects to those seen in other T Tauri populations (Feigelson & Montmerle 1999), the distribution of X-ray luminosities is quite unusual: there are too few stars with lower, but detectable, X-ray lu-

minosities given the number of stars with high luminosities. The  $\eta$  Cha luminosity function is roughly flat between  $28.5 < \log L_x < 30.5 \text{ erg s}^{-1}$ , whereas source numbers are found to rise inversely with  $\log L_X$  in well-studied pre-MS and ZAMS stellar clusters. Consider, for comparison, the Chamaeleon I young stellar cluster (Lawson, Feigelson & Huenemoerder 1996),  $\alpha$  Per (Randich et al. 1996) and the Pleiades (Stauffer, Hartmann, & Barrado Y. Navascues 1995) clusters. In these clusters, the number of X-ray sources in the range  $28.5 < \log L_x < 29.5 \text{ erg s}^{-1}$  in the *ROSAT* band is about twice the number of luminous sources with  $\log L_x > 29.5 \text{ erg s}^{-1}$ . The total stellar population, including stars undetected in X-rays, is at least 4 times the  $\log L_x > 29.5 \text{ erg s}^{-1}$  subpopulation. (This value applies for the Pleiades, where the membership catalog is most complete but still is likely missing some low-mass M and L dwarfs.)

Along an isochrone, luminosity scales with mass, and if the X-ray emission is saturated ( $L_X/L_{\text{bol}} \approx 10^{-3}$ ), then  $L_X$  should scale with mass. Indeed, Feigelson et al. (1993) reported a correlation between  $L_x$  and stellar mass in a pre-MS population such that most  $\log L_x < 29.0 \text{ erg s}^{-1}$  stars have  $M < 0.4 M_\odot$ . Extrapolating from the number of  $\eta$  Cha cluster stars with  $\log L_x > 29.5 \text{ erg s}^{-1}$  discovered in Paper I, a normal X-ray luminosity function predicts roughly 12 additional stars with  $28.5 < \log L_x < 29.5 \text{ erg s}^{-1}$  and about 16 stars with  $\log L_x < 28.5 \text{ erg s}^{-1}$ . Our HRI survey was sensitive to stars at the distance of  $\eta$  Cha with  $\log L_x > 28.5$ . We surmise that a considerable number of low-mass stars with detectable X-ray luminosities reside outside the cluster core region surveyed by *ROSAT* HRI.

Low-mass members of the cluster may have escaped after the dispersal of the proto-cluster molecular cloud. The molecular cloud core that formed the cluster stars was most likely dispersed by an external supernova or stellar winds, or possibly by the outflows and winds of the most massive cluster members. The discussion in §6 elaborates on what is known about the interstellar medium in the cluster vicinity, and points to the likely culprit being the massive stars in the Sco-Cen OB Association.

If the cluster stars formed with a small velocity dispersion of  $\approx 1 \text{ km s}^{-1}$  (as found in the Cha I molecular cloud core; Dubath, Reipurth & Mayor 1995), and the bulk of gas mass was dispersed, then the thermal motions of the stars will lead to the slow evaporation of the cluster. The escape velocity of

the cluster, from summing the modeled masses of the 13 known systems within  $15'$  (0.4 pc) radius of the center, is only  $\simeq 0.5 \text{ km s}^{-1}$  (Paper I). Doubling the cluster mass, by finding unseen companions and possible X-ray faint / low-mass stars (see §3.1), would only increase  $v_{esc}$  by  $\sqrt{2}$  to  $\simeq 0.7 \text{ km s}^{-1}$ . Numerical studies (Lada, Margulis & Dearborn 1984) show that after a bound, embedded cluster ( $N = 50\text{--}100$ ) sheds its molecular cloud, the cluster can lose 10-80% of its stars, depending on the time scale for gas dispersal and the initial star-formation efficiency. If this scenario is correct, a “halo” of low-mass members within a few degrees of the  $\eta$  Cha cluster core ( $1^\circ = 1.7 \text{ pc}$  at  $d = 97 \text{ pc}$ ), should be present.

### 3. The Stellar Population of the $\eta$ Cha cluster

#### 3.1. Initial mass function

In order to estimate the total population of the  $\eta$  Cha cluster, we extrapolate a typical IMF assuming that we have a complete census of stars with masses above a certain mass threshold. We treat the membership of stellar primaries with masses  $> 1 M_\odot$  as complete since the stars would either be in the magnitude-limited *Hipparcos* or *Tycho-2* catalogs. The *Tycho-2* catalog is 99% complete to  $V \simeq 11.0$  (Høg et al. 2000), which is 0.5 mag fainter than the  $\approx 1.0 M_\odot$  K4 star RECX 1. The HRI field has 5 primaries with model masses  $> 1 M_\odot$  ( $\eta$  Cha, RS Cha, HD 75505, RECX 1 and 7, see Table 1 of Paper I), of which only RECX 7 has no astrometric catalog entry, likely due to its proximity to HD 75505.

A coarse extrapolation of a Scalo (1998) field mass function for a population with  $5 \pm \sqrt{5}$  systems with  $M > 1 M_\odot$  predicts a total membership of  $\sim 31 \pm 14$  stellar primaries with masses greater than  $10^{-1.1} = 0.08 M_\odot$ , the canonical minimum stellar mass limit. Figure 3 displays a histogram of the masses of the known cluster stars, along with an extrapolated Scalo mass function scaled to  $5 M > 1 M_\odot$  stars. The multiplicity statistics for the  $\eta$  Cha cluster stars await future study. Assuming 1.5 stars per primary, typical for T Tauri stars in the Taurus clouds (Kohler & Leinert 1998) and young main sequence stars in the Hyades (Patience et al. 1998), our IMF extrapolation suggests a total population of  $\sim 50$  stars. Our current census includes 12 X-ray detected stars and the common proper motion A star HD 75505, so we infer that perhaps  $18 \pm 14$  additional *primaries* (i.e. systems) await discovery.

This extrapolation implies that our X-ray survey alone likely detected  $39^{+32}_{-12}\%$  of the systems in the  $\eta$  Cha core region. Did our X-ray survey miss a large number of “X-ray faint” WTTs, or have some of the cluster members dispersed outside of the field of view of *ROSAT* HRI field of view? Our discussion of the anomalous X-ray luminosity function in §2.3 suggests that many low-mass stars with detectable X-ray emission are likely to exist outside of the HRI field of view. In the next section, we also show preliminary evidence that stars with magnitudes comparable to the WTTs discovered in Paper I also exist in the core region, but were missed with HRI.

#### 3.2. Clustered X-ray faint stars

To test how complete the X-ray survey was, we examined the location of all stars selected through photometric properties. The X-ray and photometric selection have been effective complementary approaches in other pre-MS membership studies (e.g. Flaccomio et al. 1999).

Due to their proximity and youth, low-mass cluster members should appear magnitudes above the vast majority of field stars in a color-magnitude diagram (CMD). At the time of writing we were lacking accurate optical magnitudes for the cluster members, however new absolute and differential photometry (for rotation studies and HR diagram placement) will be presented in Lawson, Crause, Mamajek, & Feigelson (in preparation). For this study, we elected to use the USNO-A2.0 catalog (Monet et al. 1998) generated from the ESO/UK Schmidt photographic plates of the southern sky, which gives two-color photographic magnitudes for objects with  $F < 18$ . The photographic  $F$  magnitude is from the ESO-R IIIa-F plates, and is similar to Cousins  $R$  (Lawson, Feigelson & Huenemoerder 1996). The USNO  $B_J$  magnitudes from the UK-SRC IIIa-J plates corresponds closely to Johnson  $B$ . Using data provided by Arne Henden of USNO, we derived the following conversions: Johnson  $(B - V) = 0.863(B_J - F) + 0.005$  and Johnson  $V = F - 0.5313(B_J - F) - 0.015$ . The  $(B_J - F)$  colors were redder than what the RECX spectral types (Paper I) would predict, and the photographic magnitudes are coarse enough that we do not convert to the Johnson colors in our discussion. Although tied to the Tycho  $BV$  photometry (European Space Agency 1997), the USNO-A2.0 catalog is estimated to have absolute photometric uncertainties of  $< 0.5$  mags and relative uncertainties around 0.15 mag within a plate

in the southern hemisphere. We thus recognize that the CM diagram based on USNO magnitudes may not be a very precise tool for cluster membership study.

A  $1^\circ$  radius around  $(\alpha, \delta) = (8^h42^m, -79^\circ0')$  contains 45,058 USNO-A2.0 catalog stars. The  $(B_J - F) - F$  CM diagram for 19,747 stars with  $F < 17.5$  and  $0.5 < (B_J - F) < 5.5$  is shown in Figure 4, where the X-ray selected  $\eta$  Cha members are denoted with black circles. To isolate stars with  $F$  magnitudes not more than  $\sim 2.5$  magnitudes fainter than the X-ray stars but with similar colors, we identified 351 stars with  $F = 3.71 \times (B_J - F) + 6.86$  and  $F < 16.5$  as indicated by the dashed lines. The diagonal line approximates the location of the ZAMS at 97 pc, and the  $F = 16.5$  limit eliminates the thousands of background stars in the CM diagram. Note that the USNO magnitudes are given in 0.1 magnitude steps, hence grid-like appearance of the CMD. The celestial positions for these 351 bright red stars exhibits a clustering of tens of objects above the average stellar density within  $20'$  of the center, both in the scatter plot and in the smoothed stellar density distribution shown in Fig. 5.

To test whether the enhancement of starcounts is real<sup>5</sup>, simulations of random star positions were constructed and smoothed with various Gaussian kernels. We find that the observed enhancement is present at the  $> 3\sigma$  confidence level compared to the randomized samples. The observed variation in stellar density across the entire  $1^\circ$  field is 81% ( $1-\sigma$ ) of the average density, compared to an average of 31% ( $1-\sigma$ ) across 5 random fields. The ratio of maximum/minimum density measured in the field was 56, compared to  $11 \pm 5$  for the synthetic datasets. Examination of stars fainter than  $F = 16.5$  and to the left of the diagonal line in Figure 4 showed no statistically significant density enhancements compared to synthetic random fields.

Based on the background stellar density, we find  $\sim 50$  photometric candidates in the core region (the size of the HRI field;  $40'$ ), of which a fraction will likely be confirmed as new, low-mass members. The youth of the candidates will be tested when spectroscopy and proper motion studies are completed. The photometric study by Lawson et al. (in preparation) will address the issue of how many of the

<sup>5</sup>The clustering of the photometric candidates is unlikely to be due to extinction, as both  $\eta$  Cha and RS Cha have  $E(B - V) \simeq 0.00$  (Westin 1985, Clausen & Nordström (1980)) and the wider region is nearly dust-free (Section 5).

USNO candidates in the cluster core region are legitimate members. New WTTs discovered in the region covered by the HRI survey will either be (1) X-ray faint ( $L_X < 10^{28.5}$ ), most likely the least-luminous and lowest-mass cluster members or (2) as companions to previously known members.

#### 4. Cluster properties and comparison with other open clusters

Over 1100 open clusters are known and many have well-characterized properties such as distance, age, mass, size, concentration, metallicity and so forth (Lynga 1987; Mermilliod 1995). Table 2 summarizes the properties of the  $\eta$  Cha cluster for comparison with other clusters. The official designation format follows that of the 5th Catalogue of Open Clusters (Lynga 1987) updated to J2000 as recommended by Lortet et al. (1994). The cluster center location is estimated here from the smoothed stellar density shown in Figure 5, and agrees with the average position of the known members to within  $1'$ .

The brightest star characteristics are obtained from the *Hipparcos* catalog (European Space Agency 1997). The extinction is derived from the Stromgren photometric excess  $E(b - y) = -0.004$  reported for  $\eta$  Cha (Westin 1985). The spectral type and  $(B - V)$  color of HD 75505 imply 0.4 mags of extinction, however this is likely due to spectral misclassification (see Appendix).

The angular diameter is estimated from top panel of Figure 5; it may be underestimated if a halo of cluster members surrounds a denser core. The cluster age is from Paper I. The membership population is estimated from §3.1 and 3.2, and the  $>$  indicates that additional members may exist that have either (1) low masses and luminosities, (2) are X-ray faint or (3) are outside the HRI field-of-view. The cluster mass is estimated to be  $\approx 23 M_\odot$  from the 13 known members ( $\approx 13 M_\odot$ ) characterized in Paper I and Appendix B, plus a  $12 \pm 5 M_\odot$  contribution from  $34 \pm 14$  missing members that should exist (§3.1) with assumed average masses of  $0.35 M_\odot$  (the average mass of the stars below  $1 M_\odot$  in the extrapolated IMF shown in Fig. 3). Trumpler classifications were derived by us following the prescription of Trumpler (1930). The notation means the cluster has: detached, slight concentration (II concentration class), bright and faint stars (3 range of brightness class), and a poor population (p richness class). The radial velocity is taken

to be the weighted mean of RS Cha (Andersen 1975), RECX 1, RECX 10, and RECX 12 (Covino et al. (1997)), while  $\eta$  Cha (variable  $v_r$ ; Barbier-Brossat & Figon 2000) and RECX 7 (discordant single measurement; Covino et al. 1997) were omitted (see also §5.1). Galactic location and heliocentric velocity vector is reproduced from §5. The cluster proper motion is the weighted mean of the individual proper motions of  $\eta$  Cha, RS Cha, HD 75505, RECX 1, and RECX 11.

Comparing to the large sample of other well-characterized open clusters (Lynga 1982, Janes et al. 1988), the  $\eta$  Cha cluster has a typical central star density ( $\sim 200 M_{\odot} \text{pc}^{-3}$ ) and Z-distance from the Galactic plane for clusters of its age ( $Z = 36 \text{ pc}$ ). It is not part of any of the three established complexes of young open clusters (Perseus, Carina, Sagittarius) which are centered 1.4 – 2.3 kpc away from the Sun, but is likely associated with the Sco OB2 association (§5) which is not included in the open cluster lists.

Other properties are unusual compared to most open clusters. The brightest star is underluminous compared to other  $\sim 10$  Myr old clusters. This is probably due to the poor membership of the  $\eta$  Cha cluster compared to more distant larger clusters. The linear size of the  $\eta$  Cha cluster is also unusually small, which may be real or may indicate that we have detected only the core of a larger structure. But most striking is the proximity to the Sun: only three of  $> 1100$  open clusters are closer than  $\eta$  Cha (Fig. 8). While this is not an intrinsic property of the cluster, it makes detailed study of the characteristics of its  $\sim 10$  Myr-old stars, including very-low mass brown dwarfs, much easier to study than in other similarly-aged clusters (§7.2).

Although the  $\eta$  Cha cluster is smaller, and more poorly populated than the average open cluster in the Lynga, sample, its population and youth resemble that of the small clusters of pre-MS stars in nearby molecular clouds like Chamaleon I, Lupus, etc. Gomez et al. (1993) analyzed the spatial distributions of T Tauri stars in several nearby molecular clouds, and found that most are in clusters with memberships of tens, with cluster radii of 0.5 – 1 pc. The  $\eta$  Cha cluster has a similar inferred population and size, except that it has no molecular gas associated with it (see §6). The  $\eta$  Cha cluster therefore appears to be what a cloud core with an associated YSO population would resemble several Myr *after* the main burst of star-formation, *after* the natal molecular gas has been dispersed, but *before* the cluster has disintegrated.

## 5. Kinematics and Origin in the Sco-Cen Association

In order to investigate the origin of the  $\eta$  Cha cluster, we study the kinematics of its members and of other young stars and star-forming associations that may be related to it. Paper I mentioned that the  $\eta$  Cha cluster appeared to share proper motions with the large Lower-Centaurus Crux subgroup of the Sco OB2 (Sco-Cen) association. We consider this in detail here, and include other nearby individual and groups of young stars to investigate possibilities of a common origin. Besides the  $\eta$  Cha cluster, we include the three primary subgroups of Sco-Cen, the nearby TW Hya association, and the group of young stars near and including  $\epsilon$  Cha (details on each group are given in Appendix A).

Galactic motions and vectors were calculated using the algorithm of Skuljan, Hearnshaw & Cottrell (1999). The Sun’s current position is placed at the origin, and the UVW velocities we present are heliocentric. The algorithm factors in the parallax, position, proper motion, and the 10 *Hipparcos* covariance coefficients to produce a Galactic position and velocity with propagated uncertainties. For known widely-separated multiple stars, we use the Tycho-2 catalog, which has a much longer time baseline than the *Hipparcos* astrometry. When Tycho-2 proper motions (Høg et al. 2000) are used, the covariance coefficients are set to zero.

Our extrapolations of past stellar motion assume linear ballistic trajectories. Galactic differential rotation, the Z-direction gravitational potential, or possible gravitational deceleration by the parent molecular clouds were not included. Positional uncertainties of past locations, typically a few parsecs for individual stars, are dominated by velocity uncertainties in projection, and are ignored. These results are presented in Table 3. Note that in our discussions, weighted means are weighted by the inverse variances.

These kinematic data permit us to determine the locations of the various stars and stellar associations in the past. These results are given in Table 3. Columns 9 – 11 of Table 3 identify the Sco-Cen subgroup they were closest to in the past, along with the time and approximate distance of closest approach ( $\Delta$ ). Projected uncertainties in the past positions can be estimated from multiplying the  $1\sigma$  uncertainties in the (U,V,W) velocities times 10 Myr (1 km s<sup>-1</sup> corresponds to 1.02 pc Myr<sup>-1</sup>). The extrapolated

positional uncertainty radii 10 Myr in the past are  $\approx 10$  pc for the  $\eta$  Cha cluster, 20–30 pc for the individual TW Hya members and  $\approx 40$  pc for the TW Hya association. The past positional uncertainty radii range from 15–50 pc for members of the  $\epsilon$  Cha (the latter high value coming from the motion of  $\epsilon$  Cha itself). Owing to the large sample sizes of stars with *Hipparcos* proper motions and parallaxes (de Zeeuw et al. 1999, Z99 hereafter), we conservatively estimate the positional uncertainty radii of the Sco–Cen subgroups to be  $\leq 10$  pc.

### 5.1. Results

We find that the majority of these stars were much closer together about 10 – 15 Myr ago. Fig. 6 shows the projected current and past positions of the major associations and clusters 10 Myr in the (X,Y) plane. The solar peculiar motion of Dehnen & Binney (1998) has been subtracted, so that Fig. 6 is in the Local Standard of Rest (LSR). The  $\eta$  Cha cluster was within  $\Delta \sim 13$  pc of the centroid of the Sco–Cen LCC subgroup 11 Myr ago. The *group* motion of the 4 TW Hya members suggest that it was within  $\Delta \sim 35$  pc of the LCC 19 Myr ago. Similarly the *group* motion of the  $\epsilon$  Cha members places its centroid within  $\Delta \sim 22$  pc of the LCC about 13 Myr ago. The ages of the  $\eta$  Cha,  $\epsilon$  Cha, and TW Hya members suggest that they, too, were formed  $\sim 10$  Myr ago when they were much closer to the Sco–Cen association. . TW Hya, HD 98800, and HR 4796 are famous isolated young stars with ages of  $\approx 10$  Myr (Webb et al. 1999), and their individual motions indicate they were  $\sim 20$  pc away from Sco–Cen subgroups  $\sim 15$  Myr ago. The kinematics and HR diagram position of TWA 9 suggest it is either not a member, or the *Hipparcos* distance is too small (see Appendix A.4). Without TWA 9 factored in, the group motion of the other three TW Hya members shows they were within 28 pc of the UCL subgroup 14 Myr ago, and within 21 pc of the LCC subgroup 21 Myr ago.

We suggest that many of the TW Hya association members may have formed from a small cloud which was part of the Sco–Cen giant molecular cloud complex which formed the subgroups, but had a slightly different motion. If the HR diagram ages are to be believed, then the bulk of the star-formation in the proto-TW Hya cloud took place several Myr after the cloud was closest to the Sco–Cen complex. The same pattern is seen with the  $\eta$  Cha cluster – the HR diagram ages are several Myr younger than the time of

its closest pass to a Sco–Cen subgroup in the past.

The motions of the  $\epsilon$  Cha group stars show that they, too, are moving away from Sco–Cen. Terranege (1999) found an age of 15 Myr for RX J1159.7-7601, and we find that it was  $\Delta \sim 14$  pc of the LCC group (age: 11–12 Myr) about 16 Myr ago. We calculated a modeled age of HD 104036 of 6–7 Myr, and we find that it was  $\Delta \sim 17$  pc of the LCC group about 7 Myr ago. It appears that many young stars in this region are moving away from Sco–Cen, and their pre-MS model ages are comparable to the times when they were closest to Sco–Cen subgroups.

The motions of the Sco–Cen subgroups themselves show an interesting pattern. Curiously, the minimum pass distances between the groups are roughly equal to the nuclear age of the youngest of the two subgroups. The two oldest subgroups, LCC and UCL, were closest about 11 Myr ago ( $\Delta \sim 47$  pc versus  $d \sim 71$  pc today). The US and UCL subgroups were closest to each other  $\sim 4$  Myr ago ( $\Delta \sim 46$  pc versus  $d \sim 53$  pc today). Note that the ages derived from Walraven photometry for the subgroups are 5–6 Myr for US, 14–15 Myr for UCL, and 11–12 Myr for LCC (de Geus et al. 1989). The distances between all of the subgroup centroids are currently increasing. The 3 major subgroups of the Sco–Cen association were in a more compact configuration during their bursts of star-formation 5 – 15 Myr ago.

The times and “impact-parameters” for individual stars and the Sco–Cen subgroups have some spread, however it is clear that the groups were much closer to each other at a time when the two oldest subgroups were undergoing their bursts of star-formation. None of the groups are currently moving toward each other, and their motions appear more-or-less radial, as if they were all associated with the giant molecular cloud complex that formed the UCL and LCC subgroups 10 and 15 Myr ago, respectively.

## 6. The interstellar medium around $\eta$ Cha

Due to the youth of the  $\eta$  Cha cluster, it is possible the stars were formed in contemporary molecular clouds although it has been recognized that its immediate vicinity has no large clouds (Alcalá et al. 1995, Feigelson 1996, Mizuno et al. 1999). The Chamaeleon I cloud that has been actively forming stars for at least several million years (Lawson, Feigelson & Huenemörder 1996) lies  $8^\circ$  to the east, or  $\approx 70$  pc away three-dimensionally. The sensitive  $^{13}\text{CO}$  survey of the en-



tire Chamaeleon region by Mizuno et al. (1999) located two dozen very low-mass cloudlets around the three primary Chamaeleon molecular clouds (Cha I, II and III), each with  $\sim 10 M_{\odot}$  and a total mass of  $500 M_{\odot}$  in molecular material. But none are closer than  $\simeq 2^{\circ}$  to  $\eta$  Cha: there are no  $> 2 M_{\odot}$  clouds of gas with densities  $\geq 10^3 \text{ cm}^{-3}$  within several parsecs of the  $\eta$  Cha cluster core.

There are, however, large-scale structures in the area that may be relevant to the origin of both the Sco-Cen association and the  $\eta$  Cha cluster. A large H I filament runs parallel to the Galactic plane at  $b \simeq -25^{\circ}$ , first discovered as a “weak ridge” in an early 21-cm southern survey by McGee & Murray (1961). The feature was suggested to be the southern counterpart of the well-studied neutral hydrogen Loop I (or North Polar Spur) by Fejer & Wesselius (1973). This “Southern Hemisphere Low Velocity Filament” has a mass of order  $10^4 M_{\odot}$  and a distance around 100 – 115 pc estimated from stellar polarization studies (Cleary, Haslam & Heiles 1979, Morras 1981), similar to the *Hipparcos* distance to Lower Centaurus Crux (118 pc; Z99).

The H I filament is clearly related to a long arc of cold dust in *IRAS* far-infrared maps, as shown in Figure 7. If one interprets it as a portion of a spherical shell, the center lies around  $(\alpha, \delta) = (12^h, -63^{\circ})$  or  $(\ell, b) = (297^{\circ}, -1^{\circ})$  in the middle of the current location of the Sco-Cen LCC subgroup. de Geus (1992) discusses this in the context of various interstellar shells and loops that surround the Sco-Cen OB association. The inner “wall” of the Loop I bubble has been detected as an ISM density jump  $40 \pm 25$  pc away in the direction of Sco-Cen (Centurion & Vladilo 1991). Putting these distances into a model of a spherical bubble centered on Sco-Cen places the  $\eta$  Cha cluster within the Loop I bubble. The morphologies and distance estimates to these structure strongly suggest that past OB winds and supernova remnants from the most massive Sco-Cen stars evacuated a large volume within which the  $\eta$  Cha cluster now lies. This evacuation explains why there is very little molecular material currently present near  $\eta$  Cha, TW Hya or the other stars likely originating in the Sco-Cen giant molecular cloud. The cloudlets found by Mizuno et al. (1999) may be molecular material that has not been fully dispersed or evaporated within the hot Sco-Cen supershell.

## 7. Discussion

### 7.1. Summary

The principal results of this study are:

(1) We have convincingly established that the group of X-ray selected stars around  $\eta$  Cha constitutes a physical open cluster, and not a chance superposition of unrelated stars. In addition to the arguments in Paper I (spatial coincidence of high- and low-mass stars; identical distances and motions of the brighter stars from *Hipparcos* measurements, and a self-consistent HR diagram), we find a compact cluster of photometric candidates coincident with the X-ray-discovered population (§3, Figure 5). The  $\eta$  Cha cluster is smaller and more poorly populated than most classical open clusters (§4, Table 2). Its size and population is comparable to the small clusters seen in nearby stellar nurseries (e.g. Taurus, Lupus, etc.), but the model ages are older ( $\approx 8$  Myr) and there is no associated molecular gas or dust.

(2) The X-ray selected stars exhibit very high levels of magnetic activity, with powerful and high-amplitude X-ray variability (Table 1, Figure 2). This is supported by photometric evidence for large starspots on the stellar surfaces (Lawson et al., in preparation).

(3) The kinematics of the  $\eta$  Cha and other young stellar groupings over a large region of the southern sky indicate that many have a common origin about 10-15 Myr ago during the star-formation epochs of the Upper Centaurus Lupus and Lower Centaurus Crux subgroups of the Sco-Cen OB Association (§5, Table 3, Figure 6). In particular, both the  $\eta$  Cha cluster and TW Hya association appear to be outliers of the  $\approx 11$ -Myr-old LCC subgroup of the Sco-Cen association. We conclude that Sco-Cen is far larger than usually assumed (e.g. de Geus et al. 1989, Z99), and that more young stars or groups of stars will be found with motions consistent with an origin in or near Sco-Cen.

The presence of stellar groups like  $\eta$  Cha and TW Hya lying today  $\sim 50$  pc from the core of the Sco-Cen association can be readily understood as the consequence of their velocities inherited from the parent giant molecular cloud (Feigelson 1996). It is well-established that, on large 50 – 100 pc scales, giant molecular clouds exhibit velocity gradients and dispersions around  $5 \text{ km s}^{-1}$  (Larson 1981, Myers 1983, Efremov & Elmegreen 1998). This high velocity dispersion is usually interpreted as the consequence of

turbulence in cloud complexes. If the outlying stellar groups were unbound from the main OB association, they would have dispersed at a rate around  $5 \text{ km s}^{-1}$  for 10 Myr, which corresponds to their observed  $\sim 50 \text{ pc}$  separations from the association today.

The fate of the molecular material from which the  $\eta$  Cha stars formed is less certain. One possibility, mentioned by Jones & Herbig (1979) in another context, is that moving clouds experience resistance from the ambient medium and become separated from their newly formed stars on timescales of  $10^7$  years. But the findings reviewed in §6 suggest that the  $\eta$  Cha cluster resided in a changing interstellar environment. Initially, the cloud from which the cluster formed may have shared the stellar motion. At some later time the expanding stellar winds and/or supernova bubbles from the most massive Sco-Cen stars caught up to the cluster and evacuated or evaporated the  $\eta$  Cha cloud material.

As the H I and dust filament is just a few degrees southwest of the cluster today (Figure 7), this cloud-stripping may have occurred quite recently. If the star-formation efficiency of the  $\eta$  Cha cluster progenitor cloud was around 5 – 20%, then the cloulet was several hundred solar masses comparable to the Cha I and II clouds which are active today. It remains to be investigated astrophysically whether the Sco-Cen supernova remnants, now seen as the H I filament with  $M \sim 10^4 M_{\odot}$  could disperse a molecular cloud of this mass in the requisite time period. It is possible that the tiny molecular clouds found by Mizuno et al. (1999) throughout the Chamaeleon region are left over from this dispersal process.

The kinematic tie between the  $\eta$  Cha,  $\epsilon$  Cha, and TW Hya aggregates and the enormous Sco-Cen OB complex suggests that many of the young stars in the fourth Galactic quadrant may have their origins in the Sco-Cen giant molecular cloud. The three young stellar groups discussed here —  $\eta$  Cha,  $\epsilon$  Cha, and TW Hya — may be only a small fraction of a large population of  $\sim 10$  Myr pre-MS stars distributed in a “halo” around the main concentration of the Sco-Cen association. Some of these pre-MS stars will lie very close to the Sun.

## 7.2. Future Work

While study of the dynamical state and history of  $\eta$  Cha is beyond the scope of this paper, we can make some preliminary comments on this topic. The es-

cape velocity from the cluster is likely to be about  $\simeq 0.5 - 0.7 \text{ km s}^{-1}$  near the edge of the field that *ROSAT* HRI surveyed. Molecular clouds with several hundred masses of gas, a likely progenitor of the  $\eta$  Cha cluster, have internal three-dimensional velocity dispersions around  $1 - 2 \text{ km s}^{-1}$  (Larson 1981). If stars inherit the velocity dispersions of their progenitor molecular clouds (Feigelson 1996), then many stars may have escaped from the cluster, and the cluster core we study here may be evanescent.

The dynamical history of the cluster is probably more complex than a simple loss of high velocity stars, as it depends on the rate of gas dissipation (e.g., slow thermal evaporation or sudden removal by supernova remnants). The role of binaries and possibility of mass segregation also should be studied (e.g. Mathieu 1985, Bonnell & Davies 1998). Radial velocity measurements of more cluster members and N-body simulations are needed to address these questions with confidence. It would also be interesting to compare the dynamical evolution of  $\eta$  Cha with that of the TW Hya association, which probably had a similar origin in the Sco-Cen giant molecular cloud but is now clearly unbound and dispersed. Future kinematic simulations should also include the effects of galactic differential rotation, and the gravitational field of the disk in the Z direction.

The relative proximity of this cluster of stars, unobscured by molecular material, makes the  $\eta$  Cha cluster an ideal laboratory for studying aspects of the evolution of intermediate-aged pre-MS stars and substellar objects, such as angular momentum evolution along the Hayashi tracks, stellar multiplicity, the luminous phases of brown dwarfs, and the evolution and longevity of circumstellar disks. At a distance of 97 pc and an age of  $\sim 10$  Myr, the low-mass stellar limit is defined by  $I \approx 14$  and spectral type M5 – M6. Brown dwarfs with masses  $20 - 70 M_{Jupiter}$  are relatively bright and hot objects with  $I \approx 14 - 17$ ,  $T_{\text{eff}} = 2700 - 3100 \text{ K}$ , and spectral types M6 – M8. These are more easily located and studied than the under-luminous  $T_{\text{eff}} = 1500 - 2000 \text{ K}$ , L-type and T-type objects that characterize older brown dwarf populations (Kirkpatrick et al. 1999). Identification of additional cluster members can be provided by a combination of optical spectroscopy (spectral typing and detection of key T Tauri-star diagnostic lines such as H $\alpha$  and Li I  $\lambda 6707$ ), optical photometry and proper motion studies. The  $\eta$  Cha cluster may even be a suitable location for searching for the presence of early

planet formation; current 8 – 10-m-class instruments already allow the resolution of sub-solar system-sized structures at  $d \approx 100$  pc.

EEM thanks the J. William Fulbright program and the Australian-American Education Foundation (AAEF) in Canberra for support. WAL’s research is supported by the Australian Research Council Small Grant Scheme and University College Special Research Grants; EDF’s research is supported in part by NASA contract NAS8-38252 and NAG5-8422. This research made use of the SIMBAD database operated by the CDS in Strasbourg France, the SkyView service provided by the HEASARC at NASA-GSFC, the ESA *Hipparcos* and *Tycho* databases, the USNO-A2.0 catalog, and DENIS data obtained at the European Southern Observatory. We thank Jovan Skuljan of the University of Canterbury for graciously sharing his kinematics code in advance of publication. Thanks also go to Arne Henden (USNO) for his discussions on photographic magnitudes.

## A. Notes on the Kinematics of the Young Stars

### A.1. Kinematics of the $\eta$ Cha Cluster

Five members of the  $\eta$  Cha cluster have proper motion data from either the *Hipparcos*, *Tycho-2*, or STARNET catalogs:  $\eta$  Cha, RS Cha, HD 75505, RECX 1 and RECX 11. Only  $\eta$  Cha and RS Cha have well-determined parallaxes from the *Hipparcos* catalog, whilst HD 75505 and RECX 1 have poor *Tycho* parallaxes. Three of these systems have published radial velocity ( $v_r$ ) data:  $\eta$  Cha (Barbier-Brossat & Figon 2000), RS Cha (Andersen 1975), and RECX 1 (Covino et al. 1997).  $\eta$  Cha has a variable  $v_r$  and may be a binary; four measurements have been made ranging from  $-17$  to  $+37$  km s $^{-1}$  (Neubauer 1930, Buscombe & Morris 1961) with a mean of  $+14$  km s $^{-1}$  (Barbier-Brossat & Figon 2000).  $\eta$  Cha (B8V) was detected in our HRI survey, and we suspect the source of the radial velocity variations and variable X-ray emission is a low-mass companion. RECX 1 has  $v_r = +18 \pm 2$  km s $^{-1}$  (Covino et al. (1997)). The eclipsing binary system RS Cha was carefully monitored by several authors in order to refine the physical parameters of the system (see Appendix A, section 7). A precise radial velocity for the system,  $v_r = +15.9 \pm 0.5$  km s $^{-1}$ , is given by Andersen

(1975). RS Cha is the only system in the  $\eta$  Cha cluster which has a well-determined  $v_r$ , proper motion, and parallax producing a high-quality Galactic motion vector of (U,V,W) =  $(-12.3, -19.1, -10.6)$  km s $^{-1}$  with uncertainty  $(\sigma_U, \sigma_V, \sigma_W) = (0.8, 0.5, 0.4)$  km s $^{-1}$ .

Due to the quality of the parallaxes for both  $\eta$  Cha and RS Cha, as well as their location near the majority of cluster members WTTs, we adopt their weighted mean parallax  $\langle \pi \rangle = 10.28 \pm 0.31$  mas and Galactic position as the cluster center (X,Y,Z) =  $(34.6, -83.6, -35.9)$  pc and  $(\sigma_X, \sigma_Y, \sigma_Z) = (1.1, 2.6, 1.1)$  pc. Using the weighted mean proper motions, radial velocities, and the mean  $\langle \pi \rangle$ , we calculate the heliocentric cluster motion to be (U,V,W) =  $(-11.8, -19.1, -10.5)$  km s $^{-1}$  and  $(\sigma_U, \sigma_V, \sigma_W) = (0.6, 0.5, 0.3)$  km s $^{-1}$ . This translates into a convergent point of  $(\ell, b) = (211.7^\circ, -25.1^\circ)$  with a total space motion of 24.8 km s $^{-1}$ . This is close to the Gould’s Belt convergent point found in the RASS-Tycho-2 sample by Makarov & Urban 2000:  $(\ell, b) = (244.3^\circ, -12.6^\circ)$ , and Eggen’s (1995) Local Association or “Pleiades Supercluster”  $(\ell, b) = (240.6^\circ, -27.2^\circ)$ ;  $V_{tot} \simeq 26.5 - 0.025X$  km s $^{-1}$ ), where  $X$  is distance in the direction of the galactic center.

### A.2. Kinematics of the Sco-Cen OB association

The Sco-Cen OB association (Sco OB2) and its three primary subgroups (Upper Sco = US = Sco OB2\_2, Upper Centaurus Lupus = UCL = Sco OB2\_3, Lower Centaurus Crux = LCC = Sco OB2\_4) compromise the closest, large-scale site of recent high-mass star-formation to the Sun ( $d \simeq 118 - 145$  pc; Z99). Kinematics of the three primary subgroups of the Sco-Cen association are given by the detailed studies of Z99, de Bruijne (2000), and Hoogerwerf (2000). Z99 calculated the subgroup Galactic motions for 180 LCC, 221 UCL, and 120 US members using the median of the candidate’s radial velocities listed in the *Hipparcos* Input Catalog Turon et al. 1993.

Here, we calculate centroid positions and Galactic motion vectors to compare trajectories between these massive subgroups and other smaller groups of young stars in our discussion. Following Z99, we use mean proper motions and parallaxes, and the median subgroup radial velocities. We used the *Hipparcos* mean right ascensions, declinations, and proper motions in those two directions, for all the stars in Z99’s membership lists. We adopt their subgroup distances as de-

finned by the member candidates of all spectral types, and the median radial velocity for all of the candidate members with radial velocities in the *Hipparcos* Input Catalog. The Galactic motion vectors we calculated are purely heliocentric, and differ slightly from those of Z99 (their Table A1).

### A.3. Kinematics of stars near $\epsilon$ Cha

A kinematic group of X-ray emitting young stars at  $d \simeq 110$  pc in the vicinity of  $\epsilon$  Cha was recently discovered in Chamaeleon by Frink et al. (1998, their “subgroup 2”) and later discussed by Terranegra et al. (1999, their “kinematic group”). Eggen (1998) independently pointed out a grouping of early-type Local Association members between the Cha I, Cha II, and Musca dark clouds, at similar distances.

We combined the lists of related stars from all 3 papers and found 6 which had both *Hipparcos* astrometry and measured radial velocities, called here the “ $\epsilon$  Cha group”.  $\epsilon$  Cha AB (= HIP 58484) is a  $V = 4.9$  visual binary with a B9Vn primary. Furthermore,  $\epsilon$  Cha is comoving with the well-studied pre-MS Herbig Ae/Be star HD 104237 (age  $t \simeq 5$  Myr; Terranegra et al. 1999) located  $2.2'$  away.  $\epsilon$  Cha has  $v_r = +13 \pm 5$  km s $^{-1}$  (Barbier-Brossat & Figon 2000); however HD 104237 has no published radial velocity and was ignored in our analysis. Due to the binarity of  $\epsilon$  Cha, we adopt the Tycho-2 proper motion, but keep the *Hipparcos* parallax. Knee & Prusti (1996) detected molecular gas at  $v_r = +3.5 \pm 1.4$  km s $^{-1}$  in the close vicinity of  $\epsilon$  Cha and HD 104237 and argue that the clouds are associated with the two young early-type stars due to the high ratio of IRAS  $100 \mu\text{m}$  dust emission to CO( $J = 1 \rightarrow 0$ ) emission. The velocity of the gas is closely bracketed by the radial velocity of gas in the Cha I and Cha II clouds, which are  $d = 150\text{--}200$  pc distant (Knude & Høg 1998 and references therein). Hence the cloudlets near  $\epsilon$  Cha ( $d = 112 \pm 7$  pc; *Hipparcos*) appear to share the radial velocity of the main Cha clouds  $50 - 100$  pc beyond it, and are  $2\sigma$  below the poor radial velocity ( $\pm 5$  km s $^{-1}$ ) for  $\epsilon$  Cha in the literature. A more accurate radial velocity for  $\epsilon$  Cha and HD 104237 is desired to clear up this situation. However, for our purposes we use the Barbier-Brossat & Figon radial velocity value.

Two RASS WTTs discovered by Alcalá et al. 1995 have *Hipparcos* entries and radial velocities from Covino et al. (1997), DW Cha (=RX J1158.5-7754a, HIP 54800;  $v_r = +13.1 \pm 2.0$  km s $^{-1}$ ) and RX J1159.7-7601 (=HIP 58490;  $v_r = +13.1 \pm 2.0$  km s $^{-1}$ ),

with estimated ages of  $t \simeq 6$  Myr and 15 Myr, respectively (Terranegra et al. 1999). DW Cha is binary, so we use the Tycho-2 proper motion.

The isolated G8 “weak-line YY Orionis star” T Cha (Alcalá et al. 1993) had two published radial velocities:  $v_r = +14.6 \pm 2.1$  km s $^{-1}$  (Franchini et al. (1992)) and  $+20 \pm 2$  km s $^{-1}$  (Covino et al. (1997)), from which we adopt the weighted mean  $+17.4 \pm 1.5$  km s $^{-1}$ . Terranegra et al. (1999) find an age  $t \simeq 30$  Myr for this G8 star. Its proper motion is similar to the previously mentioned group members, however *Hipparcos* found it to be much closer ( $66_{-12}^{+19}$  pc). The galactic motion vector we compute for T Cha, (U,V,W) =  $-2.3, -18.8, -10.5$  km s $^{-1}$ , ( $\sigma_U, \sigma_V, \sigma_W$ ) =  $2.4, 1.6, 1.7$  km s $^{-1}$ , differs by  $\approx 10$  km s $^{-1}$  in the X direction from the other group members. Due to its age and discordant kinematics, we exclude it as a member and discuss it no further.

We added HD 104036 as a candidate group member (=HIP 58410, A7V,  $V = 6.7$ ), a star  $24'$  NW of  $\epsilon$  Cha and apparently codistant and comoving with it. Grenier et al. (1999) report a single observation of  $v_r = +12.4 \pm 1.0$  km s $^{-1}$  for this star, consistent with the others. On the Hertzsprung-Russell diagram, HD 104036 is above the MS, close to the RS Cha binary and HD 104237, and appears to be a  $t \simeq 6$  Myr star with  $M \approx 2 M_{\odot}$  (using D’Antona & Mazzitelli 1997 tracks).

The Galactic locations and motions for the four likely members with *Hipparcos* data and radial velocities are included in Table 3. For the average position and motion of the group, we use the position of  $\eta$  Cha as the center and the weighted mean UVW velocities of the four likely members with *Hipparcos* and  $v_{r,s}$  ( $\epsilon$  Cha, DW Cha, RX J1159.7-7601, HD 104036). The mean galactic motion vector implies that the group’s convergent point should be near  $(\ell, b) = 301.3^{\circ}, -25.8^{\circ}$ , with a mean group velocity of  $23.8$  km s $^{-1}$ . This is similar to Eggen’s Local Association or Pleiades Supercluster Eggen 1995 and the Gould Belt (Makarov & Urban 2000) (§5.1).

During our analysis, we searched a  $3^{\circ}$  radius circle around  $\epsilon$  Cha in the Tycho-2 catalog for additional comoving candidates. The four known members are spatially within  $0.5^{\circ}$  of each other, and form a tight proper motion locus. Three additional candidates were identified in the Tycho-2 catalog: the A7III/IV star HD 105234 (=HIP 59093,  $d = 106 \pm 7$  pc), the F0 star TYC 9420-676-1 (PPM 785582), and TYC 9414-191-1. HR diagram placement of HD 105234 places it

slightly above the main sequence, bringing into question its luminosity classification, but supporting the possibility of it being pre-MS. Spectroscopy of these candidates is required to test for youth to see if they are indeed related to the  $\epsilon$  Cha group.

#### A.4. Kinematics of the TW Hydrae Association

A fascinating group of nearby pre-MS stars in the fourth Galactic quadrant is the TW Hydrae association (Webb et al. 1999 and references therein). Soderblom et al. (1998) showed preliminary evidence that one of its members, HD 98800, may be kinematically linked to the Sco-Cen OB association. We incorporate four of the TW Hya group’s stars into our kinematic study – TW Hya, HD 98800, HR 4796, and TWA 9 – which have accurate *Hipparcos* proper motions and parallaxes, along with published radial velocities.

For TW Hya we adopt the very precise radial velocity presented by Torres et al. (1999) ( $v_r = +12.9 \pm 0.2$  km s<sup>-1</sup>). For HD 98800, the mean of the  $\gamma$  values from Torres et al. (1995) for the Aa+Ab and Ba+Bb pairs were used, and assigned a 0.2 km s<sup>-1</sup> uncertainty (where  $\gamma$  is the center-of-mass radial velocity of a stellar pair in an orbit solution). Due to the multiplicity of HD 98800, we use the long-baseline proper motion from the Tycho-2 catalog over the *Hipparcos* proper motion, but of course use the *Hipparcos* parallax.

For HR 4796A, we used the value given by Barbier-Brossat & Figon 2000 ( $v_r = +9.4 \pm 2.3$  km s<sup>-1</sup>) which represents the average of 7 observations. Stauffer, Hartmann, & Barrado Y. Navascues 1995 found  $v_r = +9 \pm 1$  km s<sup>-1</sup> for the M2.5 companion HR 4796B, agreeing closely with the HR 4796A value. We use the Tycho-2 proper motion since HR 4796 is binary, although it agrees well with the *Hipparcos* value.

The radial velocity for TWA 9 was reported by Torres et al. (1999):  $v_r = +9.9 \pm 0.4$  km s<sup>-1</sup>. Both TWA 9 A and B are suspiciously underluminous for Li-rich stars (see Fig. 3 of Webb et al. 1999), and their proper motions are smaller than most of the other TWA members. We propose that the *Hipparcos* parallax may be underestimating the distance to TWA 9 due to multiplicity, and  $d = 70 - 80$  pc may be more appropriate, however we retain the *Hipparcos* parallax in our calculations. The factor of 2.2 in the spread of the TW Hya stellar proper motions in Webb

et al.’s study suggest that the association has a factor of  $\sim 2.2$  depth, i.e. the members likely have distances of  $\sim 30 - 70$  pc. This is likely to be a major source of scatter in Webb et al.’s HR diagram, comparable in magnitude to the effects of stellar multiplicity.

The weighted mean locations and velocities of these three stars are given in Table 3. We treat TW Hya itself as the center of the association (this is appropriate considering the distribution of members in Webb et al.’s Fig. 2, and the mean distance of  $\sim 50$  pc). The association’s galactic motion vector is a standard mean of the values for the 4 members considered here, and is consistent with a convergent point of  $(\ell, b) = 241^\circ, -12^\circ$  and total motion of 21 km s<sup>-1</sup>. As with the  $\eta$  Cha and  $\epsilon$  Cha groups, this motion resembles that of Eggen’s Local Association or Pleiades Supercluster and the Gould Belt population.

## B. Notes on confirmed $\eta$ Cha members from Paper I

### B.1. RECX 1 = RX J0837.0–7856 = GSC 9402\_00921 = DENIS J083656.5-785646

High-resolution spectroscopy of RECX 1 indicates a K4 spectral type with a Li  $\lambda 6707$  equivalent width  $EW(\text{Li}) = 0.52\text{\AA}$  and rotational velocity  $v \sin i = 13 \pm 3$  km s<sup>-1</sup> (Covino et al. (1997)). We use the  $V$  magnitude from Tycho ( $V = 10.52$ ; European Space Agency 1997) and the bolometric correction (BC) for a K4 dwarf from Kenyon & Hartmann (1995), assuming zero reddening, to calculate the bolometric luminosity  $\log(L/L_\odot) = -0.12$ . Its  $v_r = +18 \pm 2$  km s<sup>-1</sup> (Covino et al. 1997) is similar to that for  $\eta$  Cha and RS Cha, and its space motion is parallel to  $\eta$  Cha, RS Cha, HD 75505, and RECX 11. This star had the highest X-ray luminosity of the RECX stars, and appears double ( $\approx 8''.6, 6^\circ$  NE) but saturated in the digitized Sky Survey images. The DENIS sampler (Epchtein et al. 1999) lists preliminary photometry of  $K s_{\text{auto}} = 7.22$ .

Frink et al. (1998) include the star in their proper motion subgroup #2 whose other members are all Cha I and Cha II T Tauri stars. If RECX 1 had formed in Cha I at  $d \simeq 140$  pc, it would be  $\simeq 1$  Myr old and would have traversed at least 19 pc ( $7.8^\circ$  projected), requiring a speed of at least 18 km s<sup>-1</sup> with respect to its parent cloud. Similarly, to originate in Cha II ( $d = 200$  pc), RECX 1 would be  $\sim 0.5$  Myr old and would need a relative speed of 53 km s<sup>-1</sup>. Since

RECX 1 is clearly a  $\eta$  Cha cluster member, birth in Cha I or Cha II seems implausible.

**B.2. RECX 2 =  $\eta$  Cha = HD 75416 = HR 3502 = IRASF0843-7846**

$\eta$  Cha is the brightest ( $V = 5.46$ ; Tycho) and earliest type (B8V; Houk & Cowley 1975) of the co-moving intermediate-mass stars in the cluster. Historically, the 4th edition of the Bright Star Catalogue lists  $\eta$  Cha as a member of the Sco-Cen Association (Hoffleit & Jaschek 1982), however it is well outside of the classically defined association region. Its *Hipparcos* ( $B - V$ ) color index matches that expected for a B8 star within 0.01 mags, so reddening is negligible in agreement with Stromgren photometric properties  $E(b - y) = -0.004$ ,  $\log T_{\text{eff}} = 4.107$ ,  $dM_b = 0.183$  (Westin 1985). Using the *Hipparcos* distance and  $V$  magnitude and no reddening, we calculate a luminosity of  $\log(L/L_{\odot}) = 2.02$ , placing it directly on the solar metallicity main sequence as given in both Pols et al. (1997) and Schaller et al. (1992). A  $3.8 M_{\odot}$  star reaches the main sequence with spectral type B8V in  $1 - 2$  Myr (Palla & Stahler 1993).

Mannings & Barlow (1998) found  $\eta$  Cha to be a candidate main sequence star with a debris disk or a “Vega-like source”. This is reminiscent of HR 4796A, the well-studied  $\sim 10$ -Myr-old member of the TW Hya association with an infrared excess due to circumstellar material. We found the star to be an X-ray emitter ( $\log L_X = 28.7 \text{ erg s}^{-1}$ ), unusual for late B stars (e.g. Grillo et al. 1992). Spectroscopic studies of  $\eta$  Cha found it to be a radial velocity variable ranging from  $-17 \text{ km s}^{-1}$  to  $+37 \text{ km s}^{-1}$  (Buscombe & Morris 1961, Neubauer 1930), thus it is likely a binary. The X-ray emission is likely to be produced by the lower-mass secondary rather than the intermediate-mass primary (Simon, Drake & Kim 1995).

**B.3. RECX 3 = DENIS J084137.2–790331**

The DENIS sampler (Epchtein et al. 1999) lists preliminary photometry of Gunn  $i_{\text{auto}} = 11.57$ ,  $K_{s_{\text{auto}}} = 9.47$ .

**2.4. RECX 4 = GSC 9403\_1083 = DENIS J084224.0–790403**

The DENIS sampler (Epchtein et al. 1999) lists preliminary photometry of  $J_{\text{auto}} = 9.54$ ,  $K_{s_{\text{auto}}} = 8.66$ .

**2.5. RECX 5 = DENIS J084120.1–785751**

The DENIS sampler (Epchtein et al. 1999) lists preliminary photometry of Gunn  $i_{\text{auto}} = 6.57$ ,  $J_{\text{auto}} = 7.44$ .

**2.6. RECX 7 = RX J0842.9–7904**

This star has neither a GSC or USNO-A2.0 entry, apparently due to its proximity ( $40''$  SW) to the bright binary RS Cha. Its position in Paper I was estimated from DSS, and its  $F$  magnitude was estimated from comparisons with other nearby USNO stars. On POSS-II, it appears as a visual binary (separation  $11''.4$ ,  $PA \simeq 30^\circ$ ). RECX 7 may be also be related to RECX 8 (RS Cha). The star has a double H $\alpha$  profile (Paper I) which may indicate that the star is a spectroscopic binary, or that combination of emission and absorption processes contribute to the line profile (Reipurth et al. 1996). High-resolution spectroscopy shows a K4 spectral type,  $EW(\text{Li}) = 0.46 \text{ \AA}$ , rotational velocity  $v \sin i = 28 - 32 \text{ km s}^{-1}$ , and  $v_r = +4.3 \pm 2 \text{ km s}^{-1}$  (Covino et al. (1997)). A spectral type of K3 and  $EW(\text{Li}) = 0.4 \text{ \AA}$  were derived from a lower resolution spectrum in Paper I.

**2.7. RECX 8 = RS Cha AB = HD 75747 = HR 3524**

RS Cha AB is a A8V double-lined eclipsing binary that has been well-studied since its discovery as a variable star by Strohmeier (1964). Accurate physical parameters of the binary are from a spectroscopic study by Andersen (1975) and detailed 4-color *uvby* photometry by Clausen & Nordström (1980, hereafter CN80). Andersen also suggested the  $\delta$  Scuti nature of the primary. In the comprehensive review of detached, double-lined eclipsing binary systems, Andersen (1991, hereafter A91) listed revised component masses of  $1.858 \pm 0.016$  and  $1.821 \pm 0.018 M_{\odot}$ , for A and B respectively, and temperatures  $T_{\text{eff}}(\text{A}) = 8050 \pm 200 \text{ K}$  and  $T_{\text{eff}}(\text{B}) = 7700 \pm 200 \text{ K}$ , and radii from CN80. A91 calculated identical luminosities of  $\log(L/L_{\odot}) = 1.24 \pm 0.03$  for A and B, independent of distance or bolometric correction.

In the post-*Hipparcos* era, two studies have re-examined the system as part of a sample of eclipsing binaries to test current calibrations of temperatures (Ribas et al. 1998; hereafter R98) and photometric estimates of surface gravities (Jordi et al. 1997; hereafter J97). R98 used the accurate *Hipparcos* parallax and component radii to calculate effective

temperatures of  $T_{\text{eff}}(\text{A}) = 7687 \pm 180$  K and  $T_{\text{eff}}(\text{B}) = 7331 \pm 170$  K. (Note that the R98 estimates are dependent on the bolometric corrections of Flower (1996), which are  $+0.03$  for these late A stars.) Using the CN80 photometry, J97 found  $T_{\text{eff}}(\text{A}) = 7810$  K and  $T_{\text{eff}}(\text{B}) = 7295$  K by interpolating the Strömgen-Crawford photometry and atmosphere model parameter grids of Moon & Dworetzky (1985). Although they do not give errors, we conservatively assume a 200 K uncertainty similar to those of R98 and CN80. After reviewing all of the available literature, we adopt the new J97 temperatures and the CN80 radii, and calculate new luminosities of  $\log(L/L_{\odot}) = 1.182 \pm 0.047$  for A, and  $\log(L/L_{\odot}) = 1.142 \pm 0.049$  for B (assuming  $T_{\odot} = 5781$  K as adopted by Bessell, Castelli, & Plez 1998).

All previous estimates for the age of this binary come from *post*-main sequence stellar evolution models inferring an age of  $8 - 10 \times 10^8$  yrs. Pols et al. (1997) found that “*it is not possible to fit the masses and radii of both stars [RS Cha AB] at the same age, for any metallicity,*” and that an implausible age difference of  $\sim 100$  Myr is required to reconcile the high luminosity of the secondary.

Solving the discordance in the post-MS ages, Paper I found that the system is pre-MS. We plot the system on an Hertzsprung-Russell diagram with the pre-MS evolutionary tracks of D’Antona & Mazzitelli (private communication, hereafter DM00) in Figure 9, comparing the temperatures and luminosities given by A91 and our values (labeled “New”) using the J97 temperatures and CN80 radii. DM00 kindly provided evolutionary tracks for masses  $1.7 - 2.0 M_{\odot}$  in  $0.1 M_{\odot}$  steps, and between  $5 - 9$  Myr in 1 Myr steps. We also inferred ages and masses from the isochrones of Palla & Stahler (1999; hereafter PS99). Our analysis is not meant to distinguish between the full spectrum of evolutionary models currently available, of which we have included only two, but to illustrate that the components of RS Cha are consistent with being coeval pre-MS stars.

We derive model masses from the evolutionary tracks, and give approximate  $1\sigma$  uncertainties. The upper(lower)  $1\sigma$  values of the model ages were interpolated using the edge of the  $(T_{\text{eff}}, \log(L))$  error oval closest to the next oldest(youngest) isochrone.

By interpolation of the DM00 tracks in Fig. 9 we derive model masses and ages of  $1.82 \pm 0.04 M_{\odot}$  and  $7.5 \pm 0.5$  Myr for A, and  $1.79 \pm 0.05 M_{\odot}$  and  $7.7 \pm 0.7$  Myr for B, using our new positions. With the A91

temperatures and luminosities and the DM00 tracks, we find  $1.88 \pm 0.04 M_{\odot}$  and  $7.2 \pm 0.5$  Myr for A, and  $1.88 \pm 0.05 M_{\odot}$  and  $7.0 \pm 0.5$  Myr for B. On the pre-MS tracks of PS99, we interpolated between their  $1.5 M_{\odot}$  and  $2.0 M_{\odot}$  tracks to extract masses and ages. For the A91 position on the PS99 tracks, we find  $1.85 \pm 0.03 M_{\odot}$  and  $4.7 \pm 1.0$  Myr for A, and  $1.88 \pm 0.02 M_{\odot}$  and  $3.5 \pm 0.7$  Myr for B. For our new  $(T_{\text{eff}}, \log(L))$  values on the PS tracks we find  $1.82 \pm 0.04 M_{\odot}$  and  $4.5 \pm 1.4$  Myr for A, and  $1.81 \pm 0.04 M_{\odot}$  and  $4.0 \pm 0.9$  Myr for B. The differences in the ages for the binary were nearly a factor of 2 ( $\approx 7$  Myr for DM00 and  $\approx 4$  Myr for PS99), however the masses were remarkably close to the dynamical masses of A91.

With our RS Cha HR diagram positions, the DM00 pre-MS model masses differ by  $-2\%$  from Andersen’s dynamical masses for both components, while the model masses with the A91 temperatures and luminosities are  $+1$  and  $+3\%$  higher, for A and B respectively. The PS99 model masses with the new HR diagram positions are  $0\%$  and  $3\%$  higher than the dynamical masses, and  $1\%$  and  $2\%$  lower for the A91 temperature and luminosity, for A and B respectively. Within our  $1\sigma$  model age uncertainties, the RS Cha binary is consistent with being coeval for both the DM00 and PS99 evolutionary models, thereby resolving the age discrepancy reported by Pols et al. (1997). RS Cha should be an important benchmark binary for testing evolutionary models of pre-MS intermediate mass stars.

As a tight eclipsing binary with period 1.7 days, the RS Cha system is estimated to circularize its orbit in about 5 Myr (Mayer & Hanna 1991). The orbit is observed to be circular, consistent with our age estimate of the  $\eta$  Cha cluster. Detailed modeling of the individual stars and the system dynamics may be useful in constraining pre-MS evolutionary models.

Our HRI observation of RS Cha provides one of the longest X-ray light curves of a pre-MS A star ever obtained. X-ray emission seen in some A stars, which have quiescent atmospheres that ought not generate solar-type magnetic activity, has been a mystery for nearly two decades (Simon, Drake & Kim 1995 and references therein). The RS Cha X-ray flare-like variations are quite similar to those seen in the late-type  $\eta$  Cha sources (Figure 2)<sup>6</sup>. These characteristics sug-

<sup>6</sup>RS Cha was reported at a higher level of  $3 \times 10^{30}$  erg s<sup>-1</sup> during the RASS survey (Huensch, Schmitt & Voges 1998) but

gest that RS Cha AB is actually a triple system where the X-ray emission is due to an undetected low-mass companion.

## 2.8. RECX 9

Paper I noted the star had a double  $H\alpha$  profile. As for RECX 7, this could indicate a double-lined spectroscopic binary or due to a mixture of emission and intervening absorption components (Reipurth et al. 1996).

## 2.9. RECX 10 = RX J0844.5–7846 = GSC 9403\_1279

One of the WTTs discovered with the ROSAT All-Sky Survey, this star has spectral type K7–M0,  $EW(\text{Li}) = 0.52 \text{ \AA}$ ,  $v \sin i = 9 \pm 5 \text{ km s}^{-1}$  and  $v_r = +15.0 \text{ km s}^{-1}$  (Paper I, Covino et al. 1997).

## 2.10. RECX 11 = NSV 4280 = BV 1051 = IRAS F08487–7848 = 1RXS J084659.3–785938 = GSC 9403\_1016

RECX 11 is listed in the *IRAS* Faint Source Catalogue (Moshir et al. 1989) and suspected variable star catalog (Kazarovets et al. 1998), and was detected in X-rays by the *ROSAT* All-Sky Survey (Alcalá et al. 1995) and our pointed HRI observation. The DENIS sampler (Epchtein et al. 1999) gives preliminary photometry of  $i_{\text{auto}} = 9.75$ ,  $J_{\text{auto}} = 8.76$ ,  $Ks_{\text{auto}} = 7.65$  which, assuming K7 spectral type, indicates  $\Delta(J-Ks) \simeq 0.3$  color excess. It thus appears to be a transitional Class II/III young stellar object between the classical to weak-lined T Tauri phases with a heated dusty disk but only weak  $H\alpha$  emission suggesting that active accretion has ceased. A well-studied star at a similar transitional phase, though with a younger age around 1 Myr, is HD 283447 in the Taurus cloud complex (e.g. Feigelson et al. 1994).

## 2.11. RECX 12 = RX J0848.0–7854 = GSC 9403\_0489 = DENIS J084757.1–785454

One of the 4 previously known RASS WTTs in the region, this is a M2 star with  $EW(\text{Li}) = 0.61 \text{ \AA}$ ,  $v \sin i = 13 \pm 3 \text{ km s}^{-1}$  and  $v_r = +18.0 \text{ km s}^{-1}$  (Paper I, Covino et al. 1997). The DENIS sampler (Epchtein

et al. 1999) gives preliminary photometry of Gunn  $i_{\text{auto}} = 10.63$ ,  $J_{\text{auto}} = 9.26$ ,  $Ks_{\text{auto}} = 8.36$ .

## 2.12. HD 75505 = GSC 9403\_0119

HD 75505 (Tycho  $V_T = 7.41$ , Johnson  $V = 7.39$ ) was the only bright AB star in the cluster core not detected by *ROSAT* HRI. Tycho gives a low-quality parallax  $\pi = 11.9 \pm 2.6 \text{ mas}$  or  $d = 84_{-15}^{+24} \text{ pc}$ , consistent with that of  $\eta$  Cha and RS Cha. The star is classified A1V (Houk & Cowley 1975) but its Tycho  $(B-V)_T$  color infers a Johnson color index of  $B-V = 0.158$ , about 0.13 mags redder than an unreddened A1 star (Kenyon & Hartmann 1995) but appropriate for an unreddened A6 dwarf. If the spectral type and Tycho color is correct, then HD 75505 (with  $A_V = 0.41$ ) is much more reddened than  $\eta$  Cha and RS Cha ( $A_V \simeq 0.00$ ), suggesting unrealistic clumpy extinction within the cluster core. Adopting the cluster distance  $d = 97 \text{ pc}$  and correcting for  $A_V = 0.41$  extinction, HD 75505 falls 0.05 dex in luminosity below the ZAMS (i.e. 100 Myr isochrone) for a  $\sim 2 M_\odot$  star, which is much older than the other stars in the  $\eta$  Cha cluster.

To resolve this issue, we examined the preliminary photometry from the DENIS sampler (Epchtein et al. 1999), which lists Gunn  $i_{\text{auto}} = 7.89$ ,  $J_{\text{auto}} = 7.07$ ,  $Ks_{\text{auto}} = 6.93$  for HD 75505. Assuming the DENIS  $J$  and  $Ks$  magnitudes are similar to Johnson  $J$  and  $K$ , the  $(V-J)$  and  $(V-Ks)$  colors are both consistent with unreddened A6 dwarf colors. Hence the optical and near-IR colors are both consistent with HD 75505 being an A6 dwarf. With an A6 spectral type, a distance of 97 pc, and no extinction, HD 75505 lies within 0.1 dex of  $\log(L)$  of the ZAMS in DM97’s models. Its position on the ZAMS implies a *minimum* age of about 8 – 10 Myr, consistent with the model ages of other members in Paper I.

---

this may represent confusion between RECX 8 (= RS Cha) and the X-ray brighter star RECX 7 (= RX J0842.9–7904) which is less than  $1'$  away.



## REFERENCES

- Alcalá, J.M., Covino, E., Franchini, M., Krautter, J., Terranegra, L., Wichmann, R. 1993, *A&A*, 272, 225
- Alcalá, J.M., Krautter, J., Schmitt, J.H.M.M., Covino, E., Wichmann, R., Mundt, R. 1995, *A&AS*, 114, 109
- Alcalá, J. M., Chavarria-K, C. & Terranegra, L., 1998, *A&A*, 330, 1017
- Andersen, J., 1975, *A&A*, 44, 445
- Andersen, J., 1991, *A&ARv*, 3, 91
- Barbier-Brossat, M. & Figon, P. 2000, *A&AS*, 142, 217
- Beckwith, S.V.W. & Sargent, A.I. 1996, *Nature*, 383, 139
- Béjar, V. J. S., Zapatero Osorio, M. R. & Rebolo, R., 1999, *ApJ*, 532, 671
- Bessell, M.S., Castelli, F., & Plez, B. 1998, *A&A*, 333, 231
- Bonnell, I. A. & Davies, M. B., 1998, *MNRAS*295, 691
- Bouvier, J., Forestini, M. & Allain, S., 1997, *A&A*, 326, 1023
- Brandner, W. & Koehler, R. 1998. *ApJ*, 499, L79
- Briceño, C., Hartmann, L. W., Stauffer, J. R., Gagné, M., Stern, R. A. & Caillault, J.-P., 1997, *AJ*, 113, 740
- Buscombe, W. & Morris, P. 1961, *MNRAS*, 123, 233
- Centurion, M. & Vladilo, G. 1991, *ApJ*, 372, 494
- Clausen, J. & Nordström, B. 1980, *A&A*, 83, 339
- Cleary, M.N., Haslam, C.G.T., & Heiles, C. 1979, *A&AS*, 36, 95
- Covino, E., Alcalá, J.M., Allain, S., Bouvier, J., Terranegra, L. & Krautter, J. 1997, *A&A*, 328, 187
- D'Antona, F. & Mazzitelli, I., 1994, *ApJS*, 90, 467
- D'Antona, F. & Mazzitelli, I., 1997, *Mem. Soc. Astr. Ital.*, 68, 807
- David, L. P., Harnden, F. R., Kearns, K. E. & Zombeck, M. V. 1997. "The *ROSAT* High Resolution Imager (HRI) calibration report", Smithsonian Astrophysical Observatory, [hea-www.harvard.edu/rosat/rsdc\\_www](http://hea-www.harvard.edu/rosat/rsdc_www)
- de Bruijne, J. H. J., 2000, *MNRAS*, accepted
- de Geus, E., de Zeeuw, P. & Lub, J., 1989, *A&A*, 216, 44
- de Geus, E. 1992, *A&A*, 262, 259
- Dehnen, W. & Binney, J.J. 1998, *MNRAS*, 298, 387
- de la Reza, R., Torres, C. A. O., Quast, G., & Castillo, B. V. 1989, *ApJ*, 343, L61
- de Zeeuw, P. T., Hoogerwerf, R., DeBruijne, J. H. J., Brown, A. G. A., & Blaauw, A. 1999, *AJ*, 117, 354
- Dubath, P., Reipurth, B. & Mayor, M. 1995, *A&A*, 308, 107
- Eggen, O.J. 1995, *AJ*, 110, 1749
- Eggen, O.J. 1998, "The Local Association of Very Young Stars", unpublished paper
- Efremov, Y. N., & Elmegreen, B.G., 1998. *MNRAS*, 299, 588
- Epchtein, N. et al. 1999, *A&A*, 349, 236
- European Space Agency, 1997, *The Hipparcos and Tycho Catalogues*, ESA SP-1200
- Feigelson, E. D., Casanova, S., Montmerle, T. & Guibert, J. 1993, *ApJ*, 416, 623
- Feigelson, E. D., Welty, A. D., Imhoff, C., Hall, J. C. Etzel, P. B., Phillips, R. B. & Lonsdale, C. J. 1994, *ApJ*, 432, 373
- Feigelson, E. D., 1996, *ApJ*, 468, 306
- Feigelson, E.D. & Montmerle, T. 1999. *Ann. Rev. As. Ap.*, 37, 363
- Fejes I. & Wesselius, P. 1973, *A&A*, 24, 1
- Flaccomio, E., Micela, G., Sciortino, S., Favata, F., Corbally, C., and Tomaney, A. 1999, *A&A*, 345, 521
- Flower, P. J., 1996, *ApJ*, 469, 355
- Franchini, M., Covino, E., Stalio, R., Terranegra, L., & Chavarria, K.-C. 1992, *A&A*, 256, 525
- Frink, S., Roeser, S., Alcalá, J.M., Covino, E., & Brandner, W. 1998, *A&A*, 338, 442
- Gomze, M., Hartmann, L, Kenyon, S.J., & Hewett, R. 1993, *AJ*, 105, 1927
- Grenier, S., Burnage, R., Farraggiana, R., Gerbaldi, M., Delmas, F., Gomez, A. E., Sabas, V., & Sharif, L. 1999, *A&AS*, 135, 503
- Grillo, F., Sciortino, S., Micela, G., Vaiana, G. & Harnden, F. R. Jr. 1992, *A&AS*, 81, 795
- Guillout, P., Sterzik, M. F., Schmitt, J. H. M. M., Motch, C. & Neuhäuser, R., 1998, *A&A*, 337, 113
- Harris, D. E., Silverman, J. D., Hasinger, G. & Lehmann, I. 1998, *A&AS*, 133, 431
- Hearty, T., Neuhäuser, R., Stelzer, B., Fernández, M., Alcalá, J.M., Covino, E. & Hambaryan, V. 2000, *Å*, 353, 1044.
- Herbig, G. H. 1978, in *Problems of Physics and Evolution of the Universe*, ed. L. V. Mirzoyan (Yervan:Acad. Sci. Armenian SSR), 171
- Hoffleit, D. & Jaschek, C. 1982, *The Bright Star Catalogue*, 4th ed. (New Haven:Yale Univ. Obs.)
- Høg, E., Fabricius, C., Makarov, V.V., Urban, S., Corbin, T., Wycoff G., Bastian U., Schwekendiek P., Wicenc A. 2000, *A&A*, 355, L27
- Hoogerwerf, R. 2000, *MNRAS*, 313, 43

- Houk, N. & Cowley, A. 1975, Catalogue of Two Dimensional Spectral Types for HD Stars, (Ann Arbor: Univ. Michigan)
- Huensch, M., Schmitt, J. H. M. M. & Voges, W., 1998, A&AS, 132, 155
- Janes, K. A., Tilley, C. & Lynga, G. 1988, AJ, 95, 771
- Jayawardhana, R., Hartmann, L., Fazio, G., Fisher, R. S., Telesco, C. M. & Piña, R. K., 1999, ApJ, 521, L129
- Jensen, E. L. N., Cohen, D. H., & Neuhäuser, R. 1998, AJ, 116, 414
- Jones, B. F. & Herbig, G. H. 1979, AJ, 84, 1872
- Jordi, C., Ribas, I., Torra, J., & Gimenez, A. 1997, A&A, 326, 1044
- Kazarovets, E., Samus, N. & Durlevich, O. 1998, IAU Inform. Bull. Var. Stars, 4655, 1
- Kenyon, S.J. & Hartmann, L., 1995, ApJS, 101, 117
- Kirkpatrick, J. D. et al. 1999, ApJ, 519, 802
- Knee, L.G.B. & Prusti, T. 1996, A&A, 312, 455
- Knude, J. & Høg 1998, A&A, 338, 897
- Kohler, R. & Leinert, C. 1998, A&A, 331, 977
- Lada, C.J., Margulis, M. & Dearborn, D. 1984, ApJ, 285, 141
- Larson, R. B., 1981, MNRAS, 194, 809
- Lawson, W.A., Feigelson, E.D., & Huenemoerder, D.P. 1996, MNRAS, 280, 1071
- Lortet, M.-C., Borde, S., & Ochsenbein, F. 1994, A&AS, 107, 193
- Low, F. J., Hines, D. C. & Schneider, G., 1999, ApJ, 520, L45
- Lynga, G. 1982, A&A, 109, 213
- Lynga, G., 1987, Catalogue of Open Cluster Data (5th ed.), Lund Observatory, available from the Centre des Données Stellaires, Strasbourg.
- Makarov, V.V. & Urban, S. 2000, MNRAS, in press.
- Mayer, P. & Hanna, A. M. M. 1991, Astro. Inst. Czech. Bull., 42, 98
- Mamajek, E.E., Lawson, W.A. & Feigelson, E.D. 1999, ApJ, 516, L77 (Paper I)
- Mannings, V. & Barlow, M. 1998, ApJ, 497, 330
- Martín, E.L. 1997, A&A, 321, 492
- Mathieu, R. D., 1985 in Dynamics of Star Clusters (J. Goodman & P. Hut, eds.), IAU Symp 113, 427
- Mermilliod, J.-C., 1995, in Information and On-Line Data in Astronomy (D. Egret & M.A. Albrecht, eds.) Kluwer:Dordrecht, 127. Available at [obswwww.unige.ch/webda](http://obswwww.unige.ch/webda).
- McGee, R. & Murray, J. 1961, Australian J. Phys., 14, 260
- Mizuno, A., et al., 1998, ApJ, 507, L83
- Monet, D., et al. 1998, USNO-A2.0: A Catalog of Astrometric Standards (CD-ROM)
- Moon, T.T. & Dworetzky, M.M. 1985, MNRAS, 217, 305
- Morras R. 1981, AJ, 86, 875
- Moshir, R., et al. 1989, IRAS Faint Source Catalogue, Version 2.0, (Pasadena CA:IPAC)
- Myers, P. C., ApJ, 270, 105
- Neubauer, F. 1930, Lick Obs. Bull., 429, 67
- Neuhäuser, R., 1999. Rev. Mod. Astro., in press
- Palla, F. & Stahler, S. 1993, ApJ, 418, 414
- Palla, F. & Stahler, S. 1999, ApJ, 525, 772
- Patience, J., Ghez, A.M., Reid, I.N., Weinberger, A.J., & Matthews, K. 1998, AJ, 115, 1972
- Pols, O.R., Tout, C.A., Schröder, K-P., Eggleton, P.P., & Manners, J. 1997, MNRAS, 289, 869
- Preibisch, T. 1997, As&Ap, 320, 525
- Preibisch, T. & Zinnecker, H., 1999, AJ, 117, 2381
- Prestwich, A. H., Silverman, J., McDowell, J., Callanan, P., & Snowden, S. 1998. "Spectral calibration of the ROSAT HRI", Smithsonian Astrophysical Observatory, [hea-www.harvard.edu/rosat/rsdc\\_www](http://hea-www.harvard.edu/rosat/rsdc_www)
- Randich, S., Schmitt, J. H. M. M., Prosser, C. F., & Stauffer, J. R., 1995, A&A, 300, 134
- Randich, S., Schmitt, J. H. M. M., Prosser, C. F., & Stauffer, J. R. 1996, A&A, 305, 785
- Reipurth, B., Nyman, L. A. & Chini, R. 1996, A&A, 314, 258
- Ribas, I., Gimenez, A., Torra, J., Jordi, C. & Oblak, E. 1998, A&A, 330, 660
- Scalo, J. 1998, in The Stellar Initial Mass Function, eds. G. Gilmore & D. Howell (San Francisco:ASP), 201
- Schaller, G., Schaerer, D., Meynet, G. & Maeder, A. 1992, A&AS, 96, 269
- Schatzman, E. 1962, Annales d'Astrophysique, 25, 18
- Simon, T., Drake, S. A. & Kim, P. D., 1995, PASP, 107, 1034
- Skuljan, J., Hearnshaw, J.B., & Cottrell, P.L., 1999, MNRAS, 308, 731
- Smithsonian Astrophysical Observatory. 1998. *PROS Users Guide*, Version 2.5.1, [hea-www.harvard.edu/PROS/PUG/PUG.html](http://hea-www.harvard.edu/PROS/PUG/PUG.html)
- Soderblom, D. R., et al. 1998, ApJ, 498, 385

- Stauffer, J. R., Hartmann, L. W., & Barrado Y. Navascues, D. 1995, ApJ, 454, 910
- Stauffer, J.R., Hartmann, L.W., Prosser, C.F., Randich, S., Balchandran, S., Patten, B.M., Simon, T., & Giampapa, M. 1997, ApJ, 479, 776
- Sterzik, M.F., Alcalá, J.M., Covino, E., & Petr, M.G. 1999, A&A, 346, L41
- Sterzik, M.F. & Durisen, R.H. 1995, A&A, 304, L9.
- Strohmeier, W. 1964, Inf. Bull. Var. Stars, 55
- Strom, K.M. & Strom, S.E. 1994, ApJ 424, 237
- Terranegra, L., Morales, F., Spagna, A., Massone, G., & Lattanzi, M.G. 1999, A&A, 341, L79
- Torres, G., Stefanik, R.P., Latham, D.W. & Mazeh, T. 1995, ApJ, 452, 870.
- Torres, G., Neuhäuser, R., Latham, D.W. & Stefanik, R.P. 1999, BAAS, 195, 78.07
- Torres, C.A.O., da Silva, L., Quast, G.R., de la Reza, R., & Jilinski, E. 2000, submitted to AJ.
- Trümper, J. 1983, Adv. Space Res., 2(4), 241
- Trumpler, R. J., 1930, Lick Obs. Bull, 420, 154
- Turon, C., et al. 1993. Bull. Inf. Centre Données Stellaires, ESA SP-1136, 43(5)
- Webb, R.A., et al. 1999, ApJ, 512, L63
- Westin, T. 1985, A&AS, 60, 99
- Zombeck, M. V., David, L. P., Harnden, Jr. F. R., & Kearns, K. 1995, Proc. SPIE, vol. 2518, 304
- Zuckerman, B. & Webb, R.A. 2000, ApJ, in press.

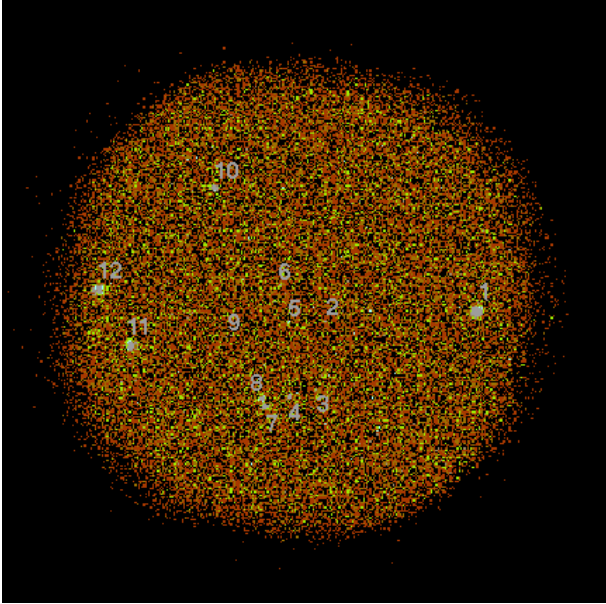


Fig. 1.— *ROSAT* HRI image of the  $\eta$  Chamaeleontis cluster. The field is centered at  $08^h42^m, -78^\circ56'$  and has a diameter of  $40'$ .

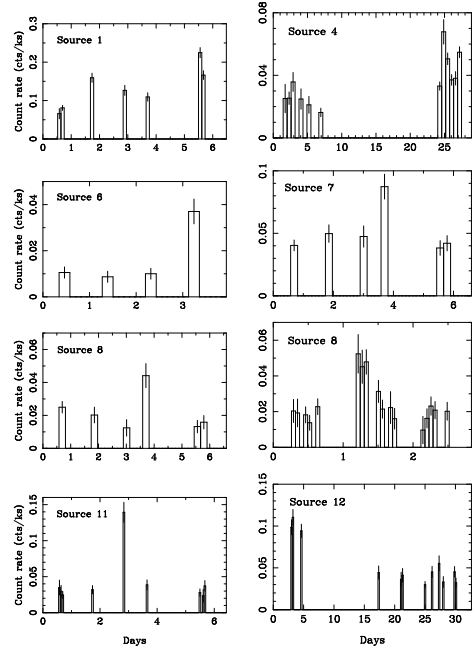


Fig. 2.— Selected X-ray light curves of highly-variable  $\eta$  Chamaeleontis stars. The source numbers refer to RECX source numbers. Starting times and bin sizes differ from panel to panel. For each source, starting times are: Source 1 (1997 October 3.2), 4 (October 3.2), 6 (April 26.5), 7 (October 3.2), 8 left (October 3.2), 8 right (October 26.5), 11 (October 3.2), 12 (September 8.9).

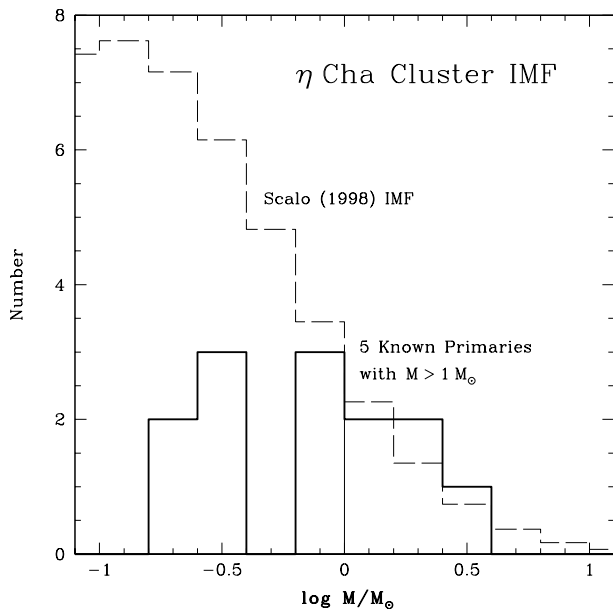


Fig. 3.— Mass function for the 12 X-ray stars and HD 75505 (thick line), compared to the Scalo (1998) initial mass function (thin line). The IMF is normalized to have five *primaries* above  $1 M_{\odot}$  (filled  $\triangle$ ). A total membership of  $31 \pm 14$  primaries is predicted, of which 13 have been discovered (see §3.1).

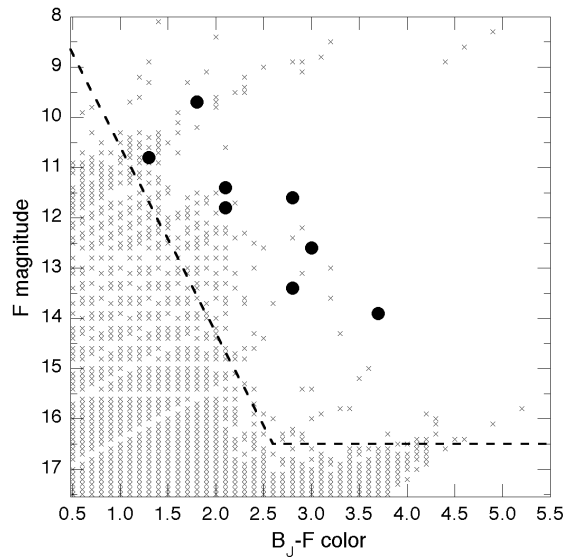


Fig. 4.— A color-magnitude diagram for 21,413 USNO A2.0 stars within a  $1^\circ$  radius of  $8^{\text{h}} 42^{\text{m}}, -79^\circ$ . The  $\eta$  Cha WTT stars are shown as large filled circles. The 351 stars selected for study in §3.2 lie above the dashed line.

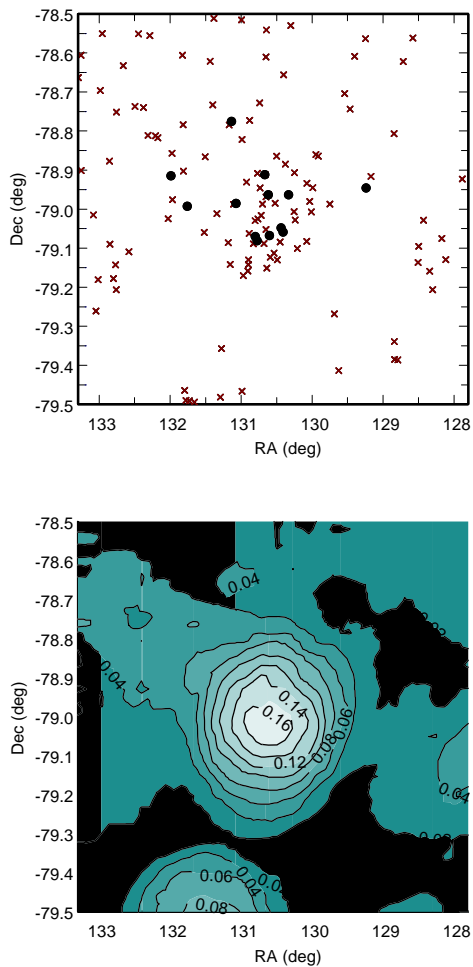


Fig. 5.— (Upper) Positions of the USNO photometric candidates (small crosses) and known  $\eta$  Cha cluster members (filled circles) in a 1 square degree box. (Lower) A density map (stars arcmin<sup>-2</sup>) of these stars smoothed with a 20' diameter kernel.

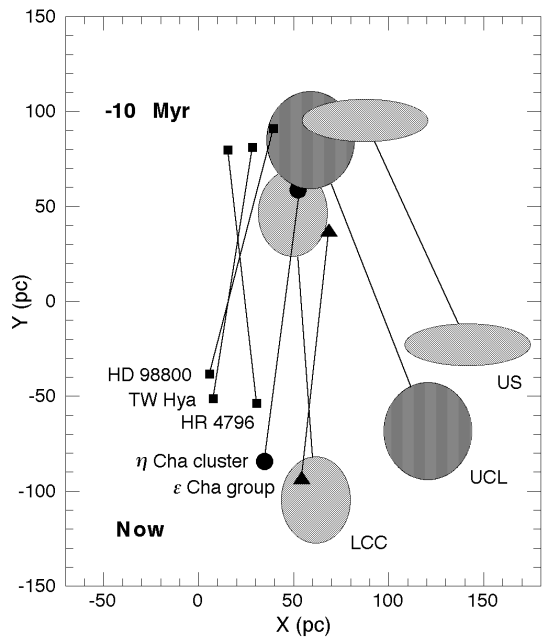


Fig. 6.— The Galactic positions of the  $\eta$  Cha cluster, TW Hydra association, the  $\epsilon$  Cha group, and Sco-Cen OB subgroups now and projected back 10 Myr ago based on Table 3. The motions are with respect to the LSR; the solar peculiar motion (Dehnen & Binney 1998) has been subtracted. The shapes of the Sco-Cen subgroups reflect their 3D extent, with the radii in X and Y being one standard deviation of the positions of all of the subgroup members as given by Z99.

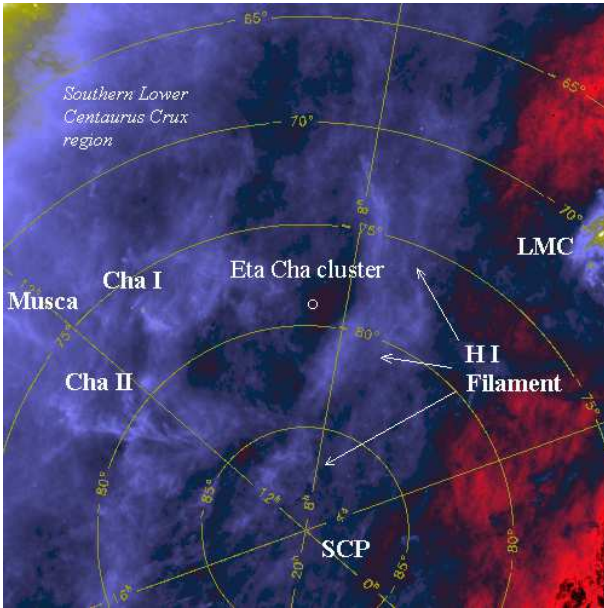


Fig. 7.— *IRAS* 100  $\mu\text{m}$  image, 30° in extent, of the  $\eta$  Cha cluster vicinity. The dust feature associated with the H I filament, important molecular clouds in the region, and the Sco-Cen LCC current location are indicated.

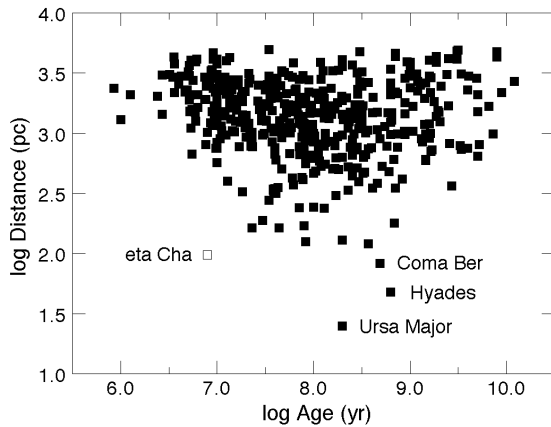


Fig. 8.— Comparison between the  $\eta$  Cha cluster and 480 clusters with  $d < 5000$  pc (Mermilliod 1995) showing it is unusually close and young.

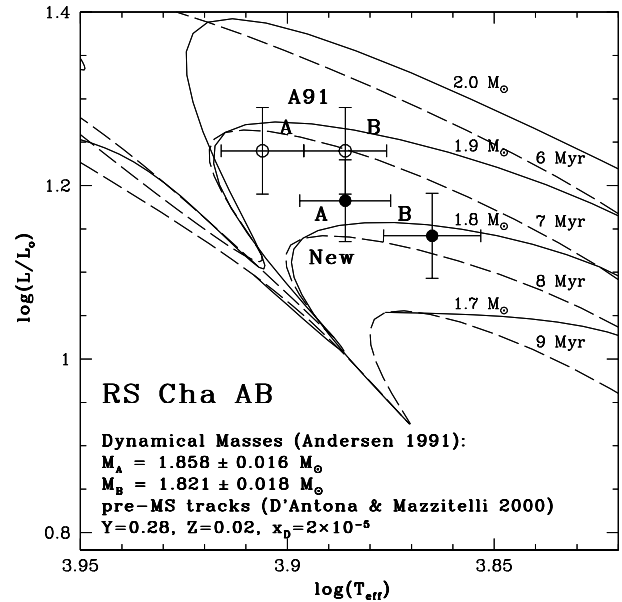


Fig. 9.— Theoretical HR diagram position for the components of the RS Cha eclipsing binary system. The isochrones of DM00 are overlaid. The difference between the Andersen (1991) positions and the new positions we calculated are that we used the temperatures of Jordi et al. (1997; J97) (see Appendix B.7). The dynamical masses and pre-MS model masses agree within 3% for the tracks of DM00 and PS99. The system appears to be a coeval pre-MS binary with age estimates of 7–8 Myr (DM00) or 4–5 Myr (PS99).

TABLE 1  
*ROSAT*  $\eta$  CHA X-RAY SOURCES

RECX (1)	Count rate		$\log(L_X)^a$ erg s $^{-1}$	Stellar counterpart (5)	Offset " (6)	Variability cts ks $^{-1}$ (7)	USNO photometry	
	cts ks $^{-1}$ (2)	$\pm$ (3)					$B_J$ (8)	$F$ (9)
1	105	2	30.6	GSC 9402_0921	2.1	Yes (0.08–0.22)	11.5	9.7
2	1.2	0.3	28.8	$\eta$ Cha	0.9	No	... <sup>c</sup>	... <sup>c</sup>
3	3.2	0.4	29.2	USNO-A2.0	1.2	No	12.6	14.0
4	32	1	30.2	GSC 9403_1083	1.5	Yes (0.01–0.04)	14.4	11.6
5	2.5	0.3	29.1	USNO-A2.0	1.6	No	17.6	13.9
6	8.2	0.5	29.6	GSC 9403_0288	3.6	Yes (0.01–0.04)	15.6	12.6
7	50	1	30.4	anonymous	2.7	Yes (0.04–0.09)	... <sup>d</sup>	10: <sup>d</sup>
8	17.0	0.7	29.9	RS Cha	2.8	Yes (0.01–0.05)	... <sup>c</sup>	... <sup>c</sup>
9	0.6	0.3	28.5	USNO-A2.0	1.0	No	15.2	13.4
10	17.9	0.8	30.0	GSC 9403_1279	3.7	Possible	13.5	11.4
11	32	1	30.2	GSC 9403_1016	3.3	Yes (0.02–0.14)	12.1	10.8
12	33	1	30.2	GSC 9403_0389	4.0	Yes (0.02–0.11)	13.9	11.8
...	<i>b</i>	<i>b</i>	<i>b</i>	GSC 9398_0105	<i>b</i>	<i>b</i>	12.3	11.6

<sup>a</sup>Log ( $L_x$ ) values are 0.1 above those reported in Paper I due to an earlier error in determining the exposure time corrections.

<sup>b</sup>Faint source close to northern edge of HRI field where exposure time is uncertain due to satellite dithering. The optical counterpart is too faint and blue to be a cluster member, hence we do not assign it an RECX number.

<sup>c</sup>Unreliable magnitudes from Sky Survey Schmidt plates due to saturation.

<sup>d</sup>Star is not listed in catalogs due to proximity to RS Cha.  $F$  magnitude is estimated by visual inspection of DSS.



TABLE 2  
 $\eta$  CHA CLUSTER PROPERTIES

Property (1)	Value (2)
Designation	C J0842-790
Location (J2000)	8 <sup>h</sup> 42 <sup>m</sup> 06 <sup>s</sup> , -79° 01' 38''
(Galactic)	292.48°, -21.65°
Parallax (distance)	10.28 ± 0.31 mas (97.3 ± 3.0 pc)
Brightest star	$\eta$ Cha, $V = 5.46$ , B8V
$E(B - V)$	0.00
Angular (linear) diameter	40': (1.2: pc)
log(Age) (yr)	6.9 ± 0.3
Membership	50? (known primaries: 13)
Mass	~ 23 $M_{\odot}$ (known members: 13 $M_{\odot}$ )
Trumpler class	II3p
Proper motion ( $\alpha$ )	$\mu_{\alpha} = -30.0 \pm 0.3$ mas yr <sup>-1</sup>
Proper motion ( $\delta$ )	$\mu_{\delta} = -27.8 \pm 0.3$ mas yr <sup>-1</sup>
Radial velocity	+16.1 ± 0.5 km s <sup>-1</sup>
Heliocentric Position (X,Y,Z)	(+35, -84, -36) pc
Heliocentric Velocity (U,V,W)	(-11.8, -19.1, -10.5) km s <sup>-1</sup>

TABLE 3  
GALACTIC POSITIONS AND KINEMATICS OF YOUNG STARS AND STELLAR SYSTEMS AROUND CHAMAELEON

Object (1)	X, $\sigma_X$ (pc) (2)	Y, $\sigma_Y$ (pc) (3)	Z, $\sigma_Z$ (pc) (4)	U, $\sigma_U$ $\text{km s}^{-1}$ (5)	V, $\sigma_V$ $\text{km s}^{-1}$ (6)	W, $\sigma_W$ $\text{km s}^{-1}$ (7)	Age <sup>a</sup> (Myr) (8)	Closest Group (9)	Time (Myr) (10)	$\Delta$ (pc) (11)
<i><math>\eta</math> Cha Cluster Members</i>										
<i><math>\eta</math> Cha</i>	34.3(1.4)	-83.3(3.5)	-35.8(1.5)	-12.2(3.6)	-17.2(8.6)	-9.6(3.7)	MS	LCC	-10	24
RS Cha	34.9(1.6)	-83.9(3.8)	-36.0(1.6)	-12.3(0.8)	-19.1(0.5)	-10.6(0.4)	8	LCC	-10	17
RECX 1 <sup>b</sup>	34.2(1.0)	-83.6(2.5)	-36.2(1.1)	-10.3(1.2)	-20.4(1.8)	-11.1(1.1)	6	LCC	-11	24
<i>TW Hya Association Members</i>										
TW Hya	7.8(1.0)	-51.4(6.4)	22.0(2.7)	-12.0(1.8)	-18.2(0.9)	-5.0(1.4)	10	LCC	-14	23
HD 98800	5.7(0.8)	-38.4(5.1)	26.0(3.5)	-13.3(1.9)	-17.9(1.4)	-6.9(1.6)	10	US	-16	18
HR 4796	30.6(1.5)	-53.7(2.7)	26.1(1.3)	-8.5(1.3)	-18.3(1.9)	-3.6(1.0)	8 $\pm$ 2	UCL	-18	28
TWA 9 (CD-36 <sup>o</sup> 7429)	15.2(1.8)	-43.5(5.2)	20.2(2.4)	-7.0(1.3)	-15.2(0.9)	-3.0(1.0)	?	LCC	-6	63
<i><math>\epsilon</math> Cha Group Candidate Members</i>										
DW Cha	41.5(4.6)	-71.7(8.0)	-22.7(2.5)	-7.9(2.1)	-17.8(1.9)	-7.9(1.2)	6	UCL	-14	38
RXJ 1159.7-7601	44.6(7.1)	-78.0(12.4)	-21.5(3.4)	-8.8(2.6)	-18.2(2.0)	-8.5(1.2)	15	LCC	-16	14
HD 104036	51.1(2.8)	-88.3(4.9)	-27.8(1.5)	-12.2(1.1)	-18.1(0.9)	-11.9(0.6)	6-7	LCC	-7	17
$\epsilon$ Cha (HD 104174)	54.1(3.5)	-93.0(6.0)	-30.1(2.0)	-11.4(2.8)	-18.0(4.2)	-10.7(1.5)	5?	UCL	-10	40
<i>Clusters/Associations</i>										
<i><math>\eta</math> Cha Cluster<sup>c</sup></i>	34.6(1.1)	-83.6(2.6)	-35.9(1.1)	-11.8(0.7)	-19.1(0.5)	-10.5(0.3)	8 $\pm$ 4	LCC	-11	13
TW Hya Assn.	54:	-93:	-30:	-10.2(2.9)	-17.4(1.5)	-4.6(1.8)	$\approx$ 10	LCC	-19	34
$\epsilon$ Cha Group	48:	-83:	-26:	-10.2(2.2)	-18.6(1.1)	-8.8(2.1)	$\approx$ 5-15	LCC	-13	22
Lo. Cen. Crux (LCC)	61.6(17.7)	-102.5(23.0)	13.8(15.9)	-8.8	-20.0	-6.2	11-12	UCL	-11	47
Up. Cen. Lup. (UCL)	121.8(29.8)	-68.6(25.8)	32.3(16.4)	-3.9	-20.3	-3.4	14-15	US	-4	46
Up. Sco. (US)	141.2(34.3)	-21.8(10.8)	49.9(16.1)	-4.7	-16.8	-6.7	4-5	UCL	-4	46

<sup>a</sup> Ages of  $\eta$  Cha stars from Paper I, Sco-Cen subgroups from de Geus et al. (1989), TW Hya and TWA 9 from Webb et al. (1999), HD 98000 from Soderblom et al. (1998), HR 4796 from Stauffer et al. (1995), T Cha, DW Cha, RX J1159.7-7601 from Terranegra et al. (1999), HD 104036 and  $\epsilon$  Cha are from isochrone fitting done by us using D'Antona & Mazzitelli 1997 pre-MS models. UVW galactic motion vectors are calculated using *Hipparcos* and Tycho-2 astrometry and radial velocities in the literature; see Appendix A for references.

<sup>b</sup> To calculate the position and velocity of RECX 1, we assumed  $\pi$  to be the weighted mean of the individual parallaxes for RS Cha and  $\eta$  Cha.

<sup>c</sup>  $\eta$  Cha cluster mean position is weighted mean for  $\eta$  Cha and RS Cha; cluster mean velocity is calculated in Appendix A.1